Electronic Supplementary Information (ESI) for RSC Advances

Synthesis and evaluation of photophysical, electrochemical, and ROS generation properties of new chalcogen-naphthoquinones-1,2,3-triazoles hybrids

Luana S. Gomes,[a] Érica O. Costa,[a] Thuany G. Duarte,[a] Mateus H. Köhler,[b] Bruna M. Rodrigues,[d] Vitor F. Ferreira,[c] Fernando C. da Silva,[d] Bernardo A. Iglesias,[e,*] and Vanessa Nascimento[a,*]

[a]SupraSelen Laboratory, Department of Chemistry, Federal University Fluminense, Institute of Chemistry, Campus do Valonguinho, 24020-141, Niterói-RJ, Brazil; [b]Department of Physics, Federal University of Santa Maria, 97105-900, Santa Maria-RS, Brazil; [c]Faculty of Pharmacy, Department of Pharmaceutical Technology, 24241-000, Niterói-RJ, Brazil; [d] Laboratório de Síntese Orgânica Aplicada (LabSOA), Institute of Chemistry, Universidade Federal Fluminense, 24020-141, Niterói-RJ, Brazil.; [e]Bioinorganic and Porphyrin Materials Laboratory, Department of Chemistry, Federal University of Santa Maria, 97105-900, Santa Maria-RS, Brazil.

^{1}H, ^{13}C NMR Spectra and HRMS (APPI+)

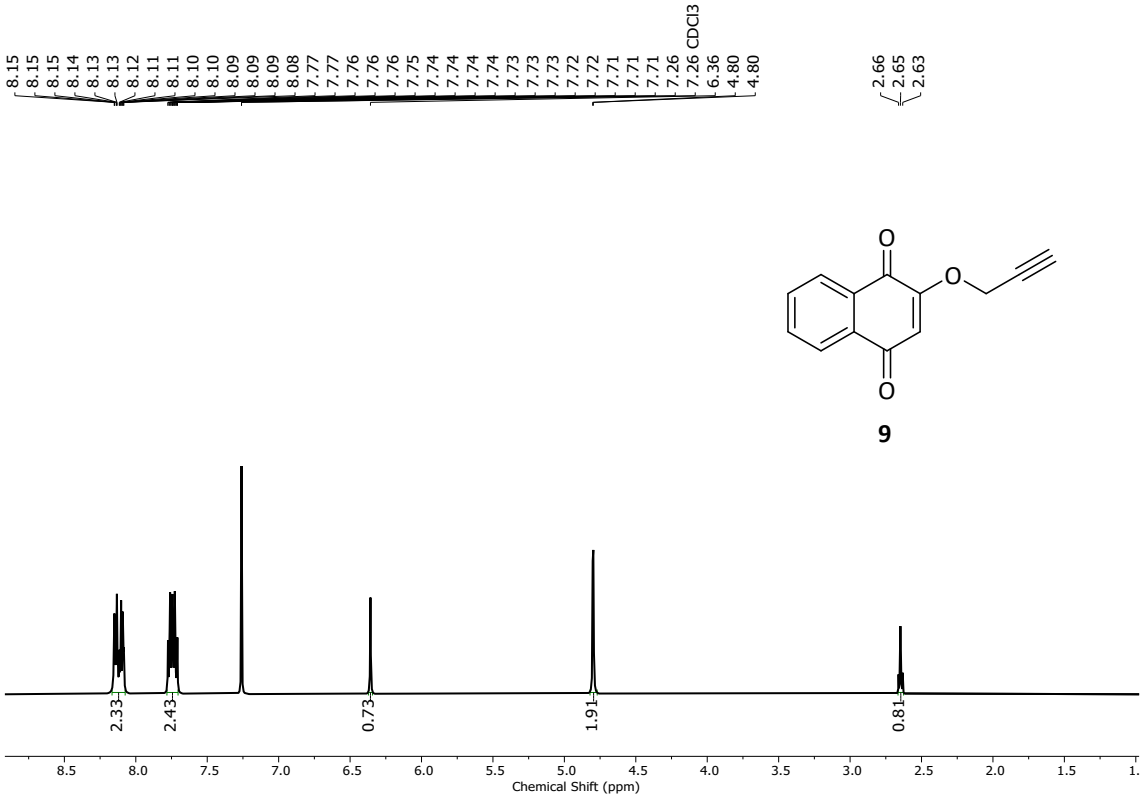

Figure S1. ^{1}H NMR spectrum of compound **9** in $CDCl_3$ at 500 MHz.

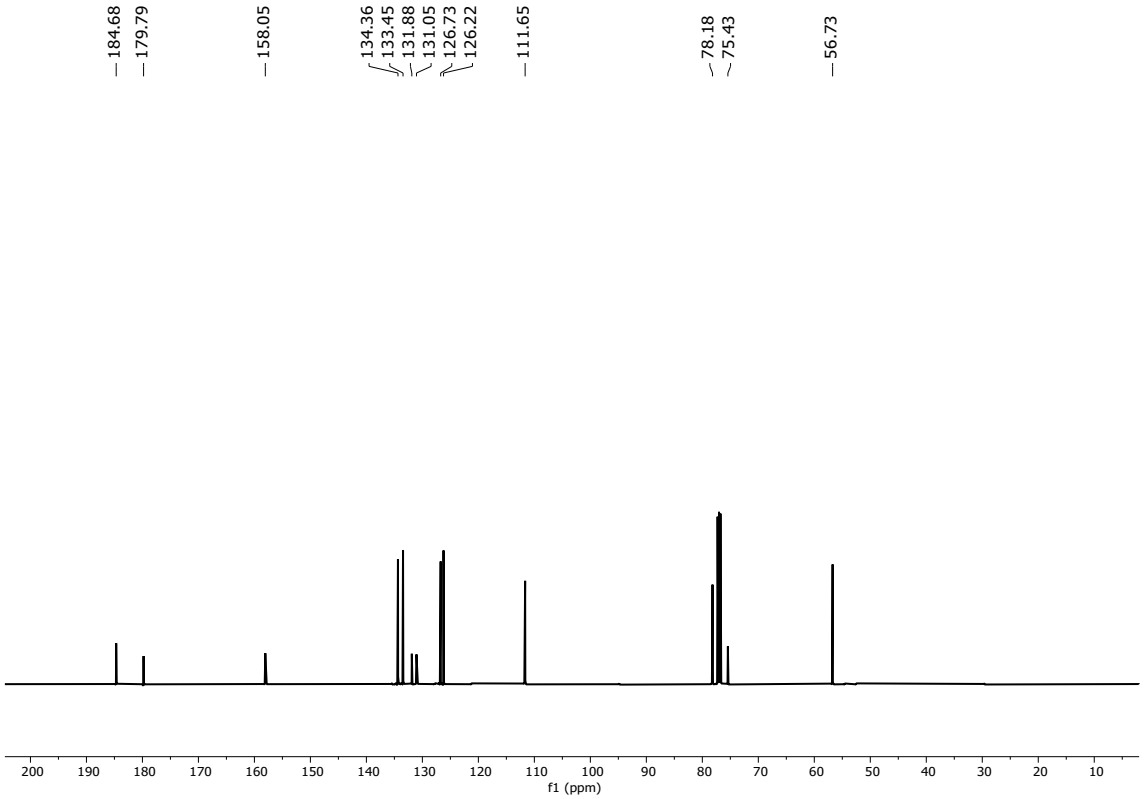

Figure S2. ^{13}C NMR spectrum of compound **9** in $CDCl_3$ at 125 MHz.

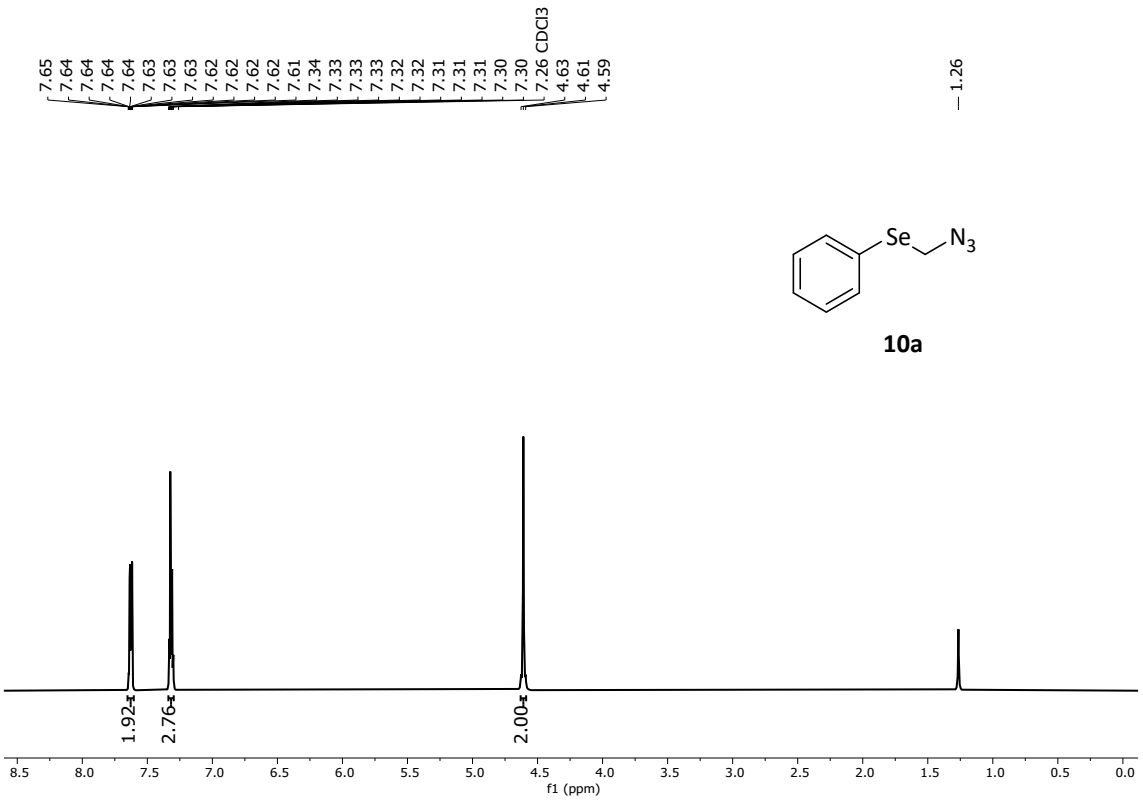

Figure S3. ^{1}H NMR spectrum of compound **10a** in $CDCl_3$ at 500 MHz.

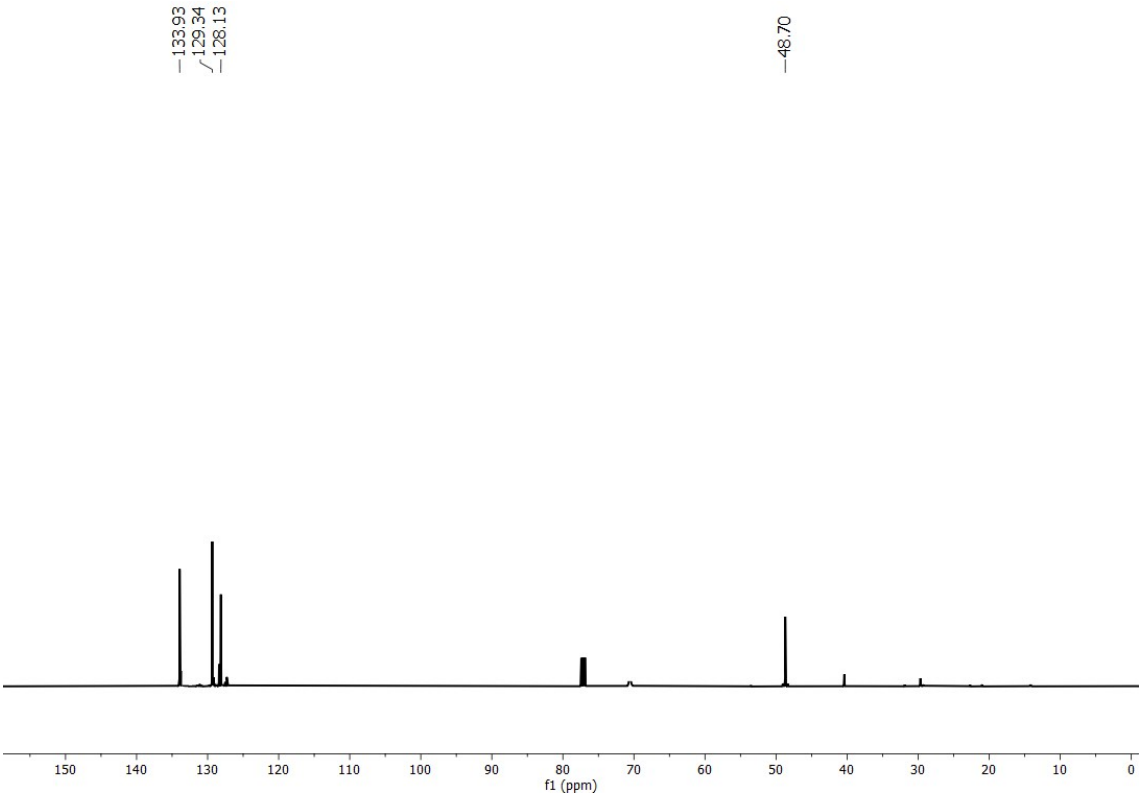

Figure S4. ^{13}C NMR spectrum of compound **10a** in $CDCl_3$ at 125 MHz.

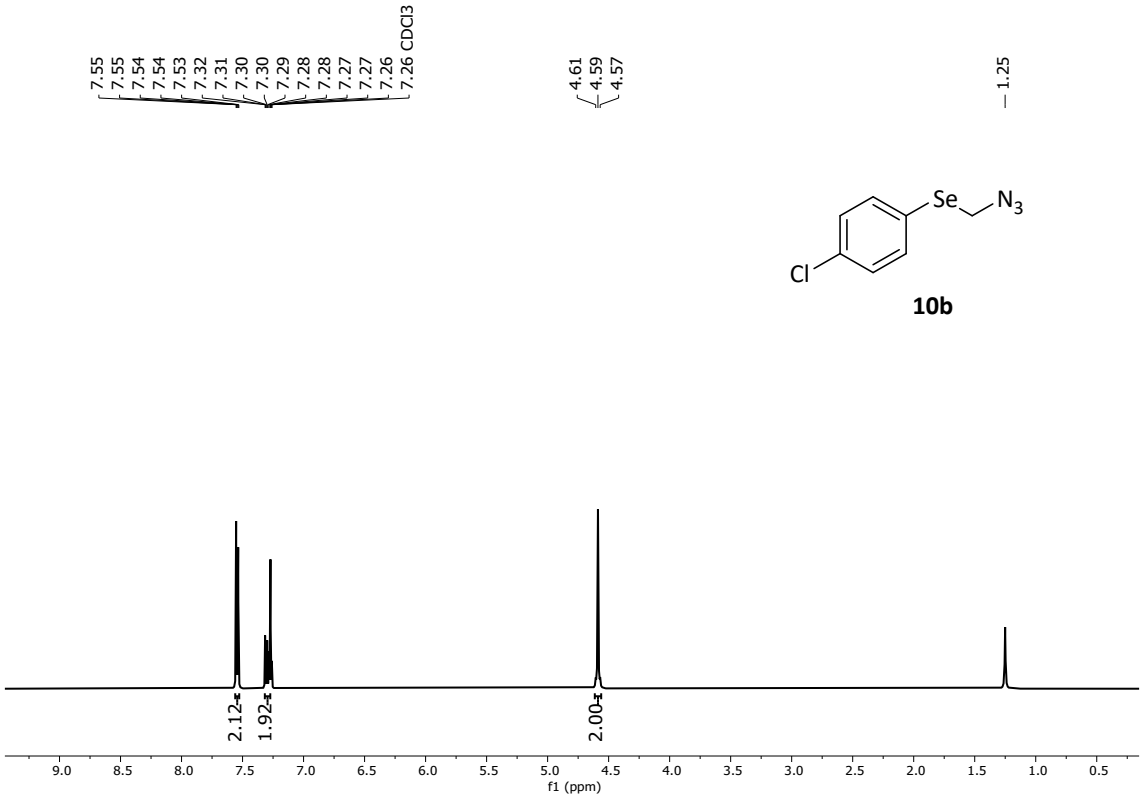

Figure S5. ^{1}H NMR spectrum of compound **10b** in $CDCl_3$ at 500 MHz.

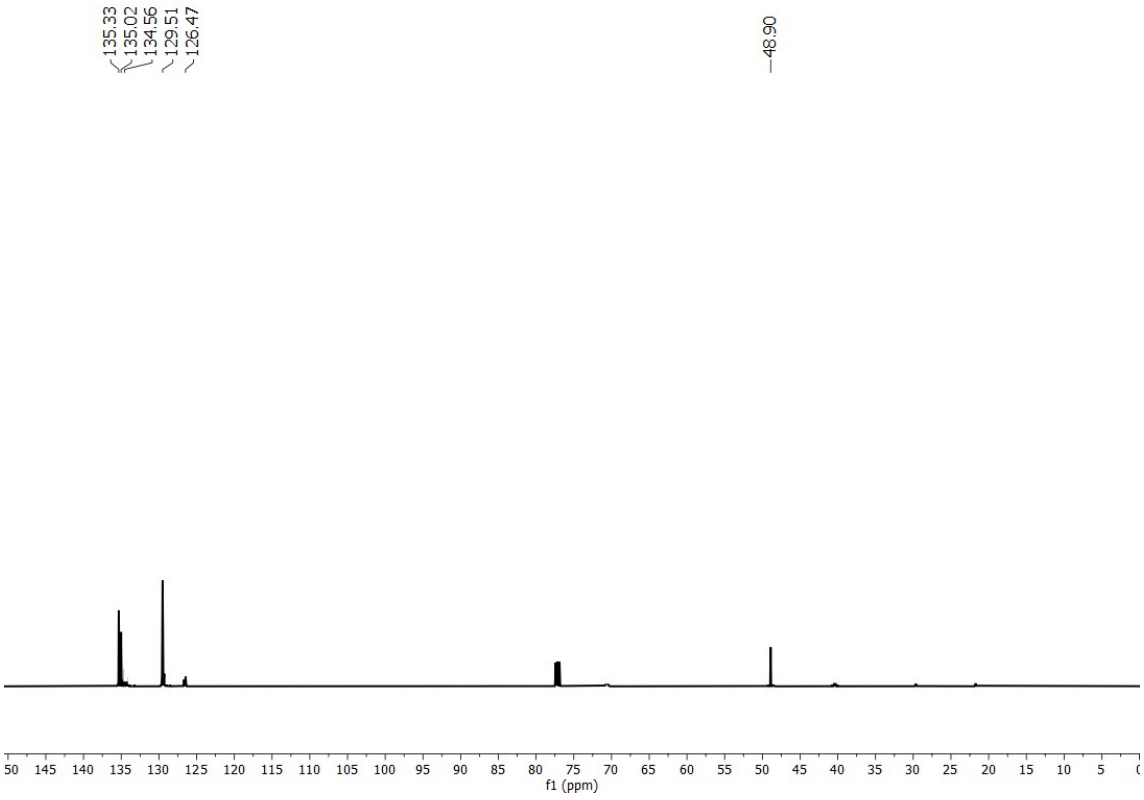

Figure S6. ^{13}C NMR spectrum of compound **10b** in $CDCl_3$ at 125 MHz.

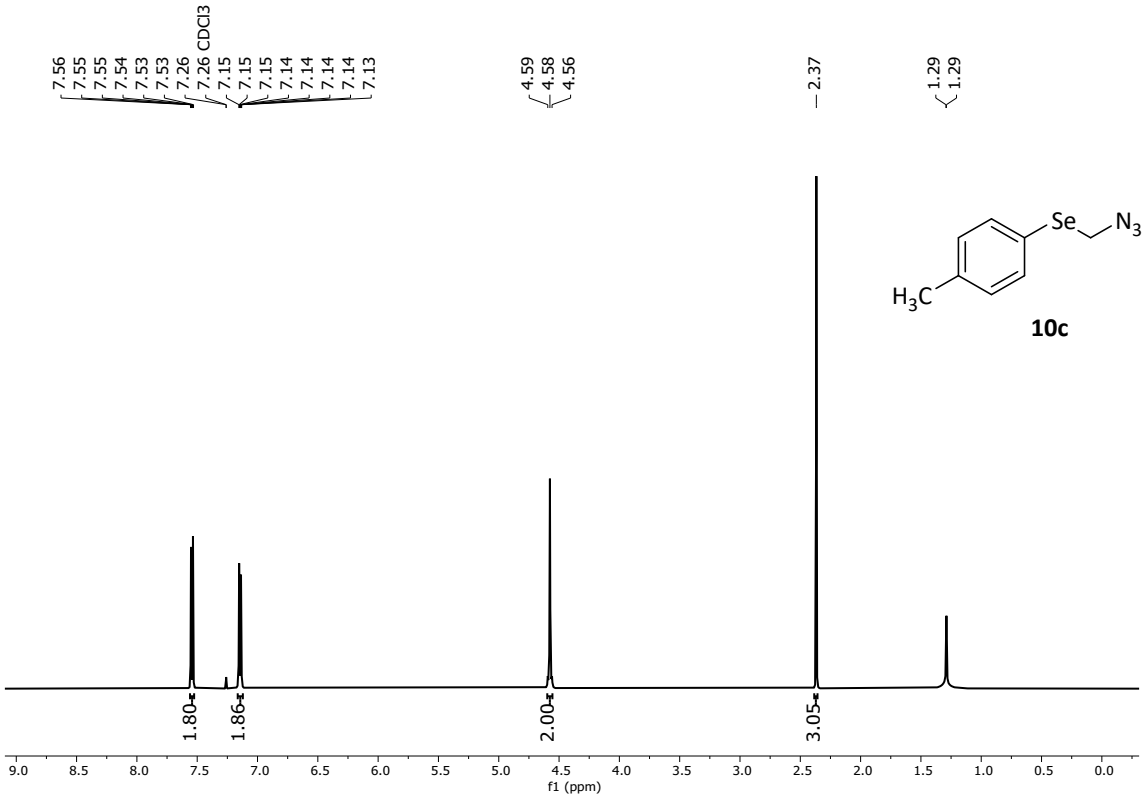

Figure S7. ^{1}H NMR spectrum of compound **10c** in $CDCl_3$ at 500 MHz.

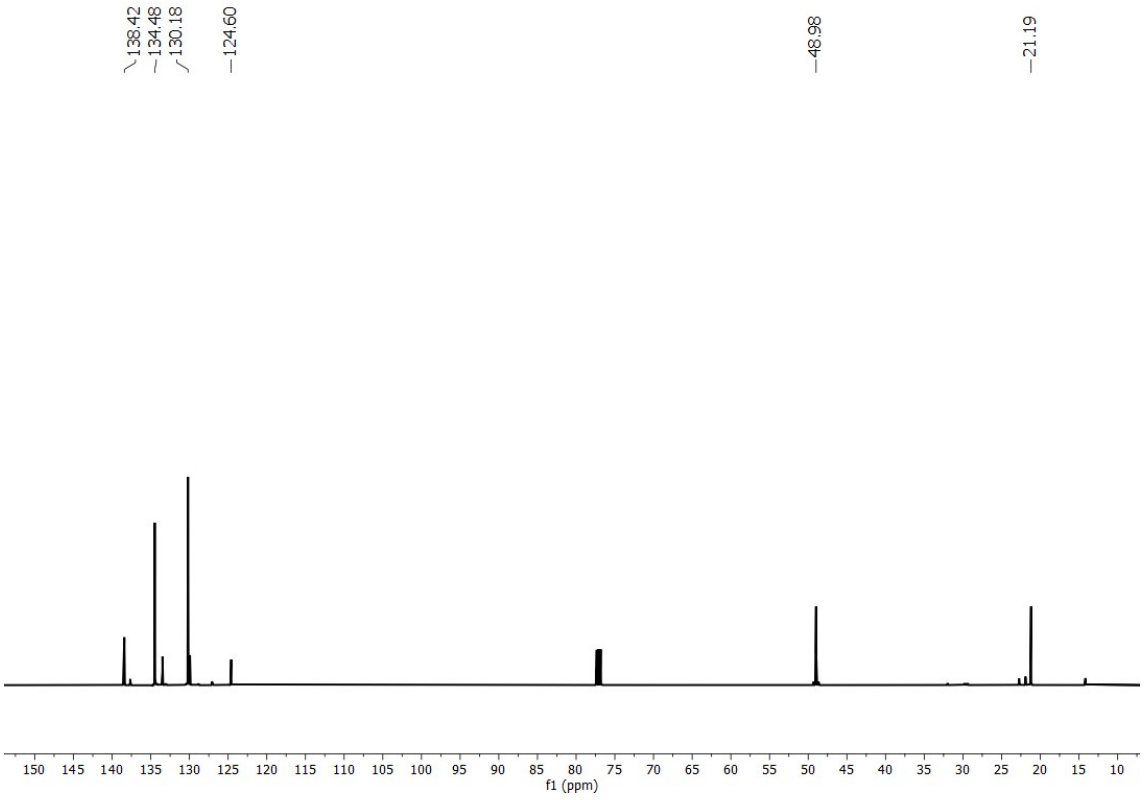

Figure S8. ^{13}C NMR spectrum of compound **10c** in $CDCl_3$ at 125 MHz.

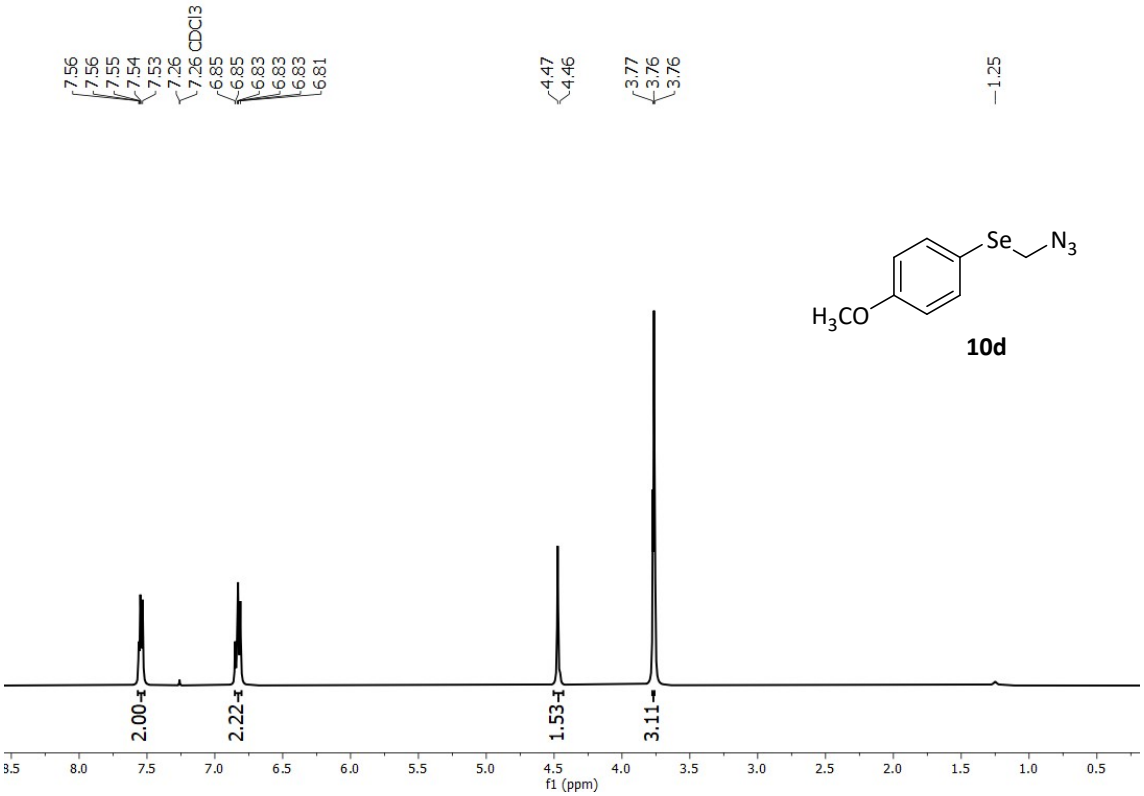

Figure S9. ^{1}H NMR spectrum of compound **10d** in $CDCl_3$ at 500 MHz.

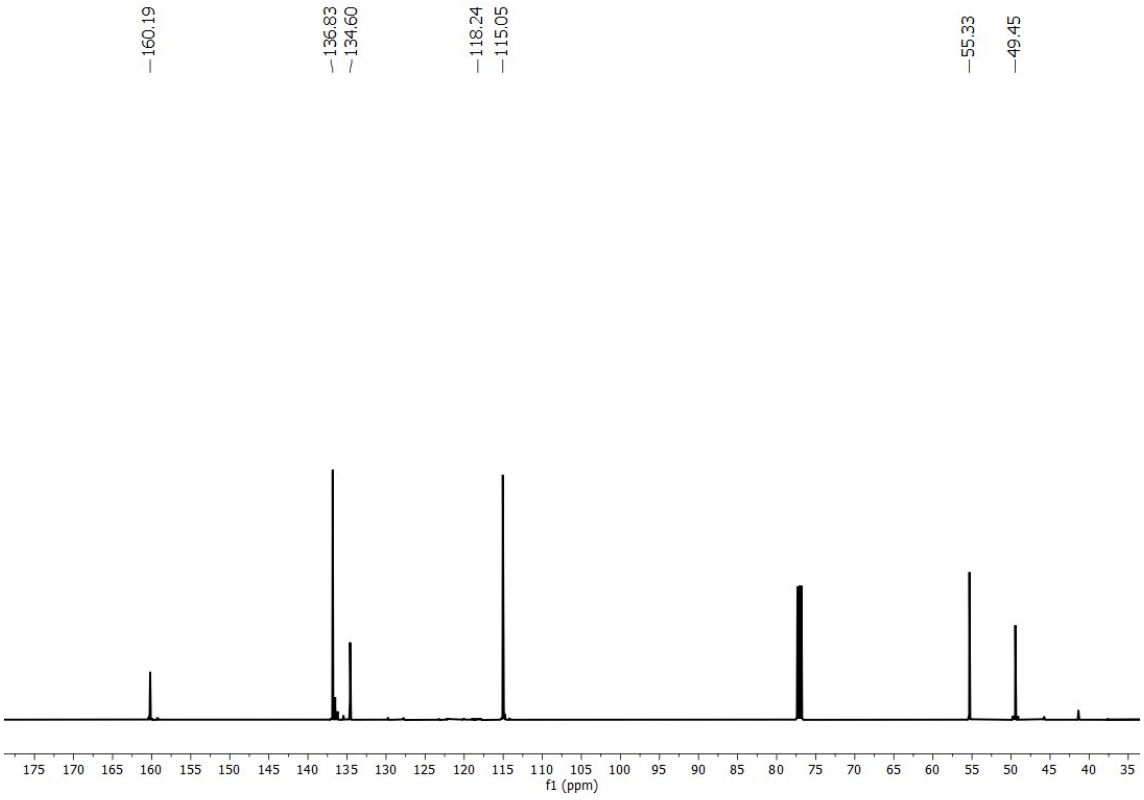

Figure S10. ^{13}C NMR spectrum of compound **10d** in $CDCl_3$ at 125 MHz.

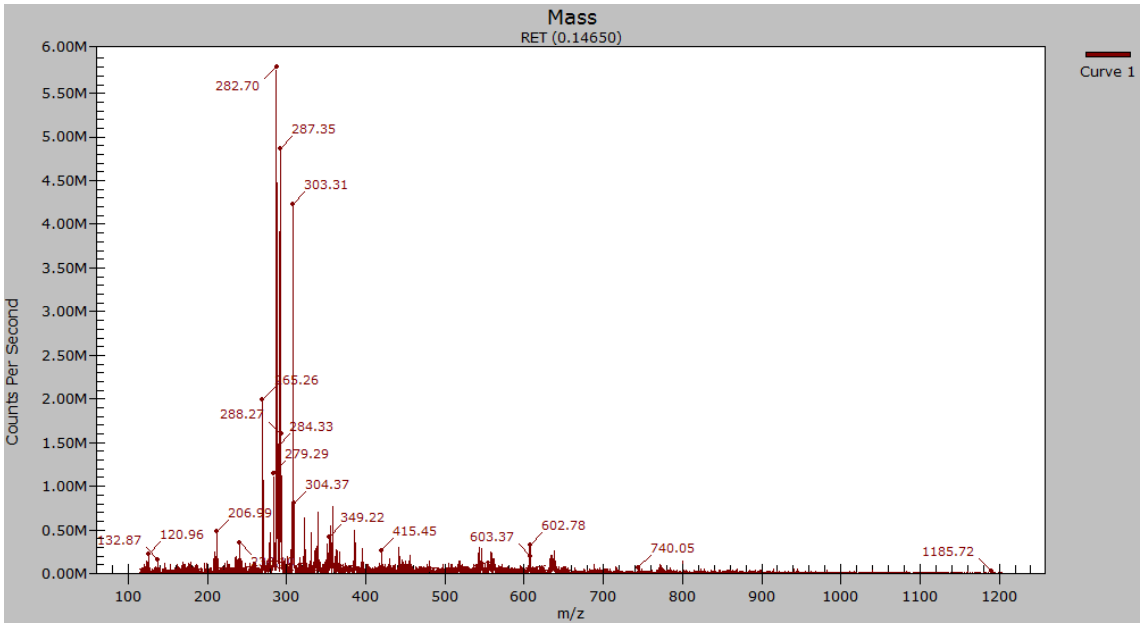

Figure S11. ESI MS spectrum of **10d**.

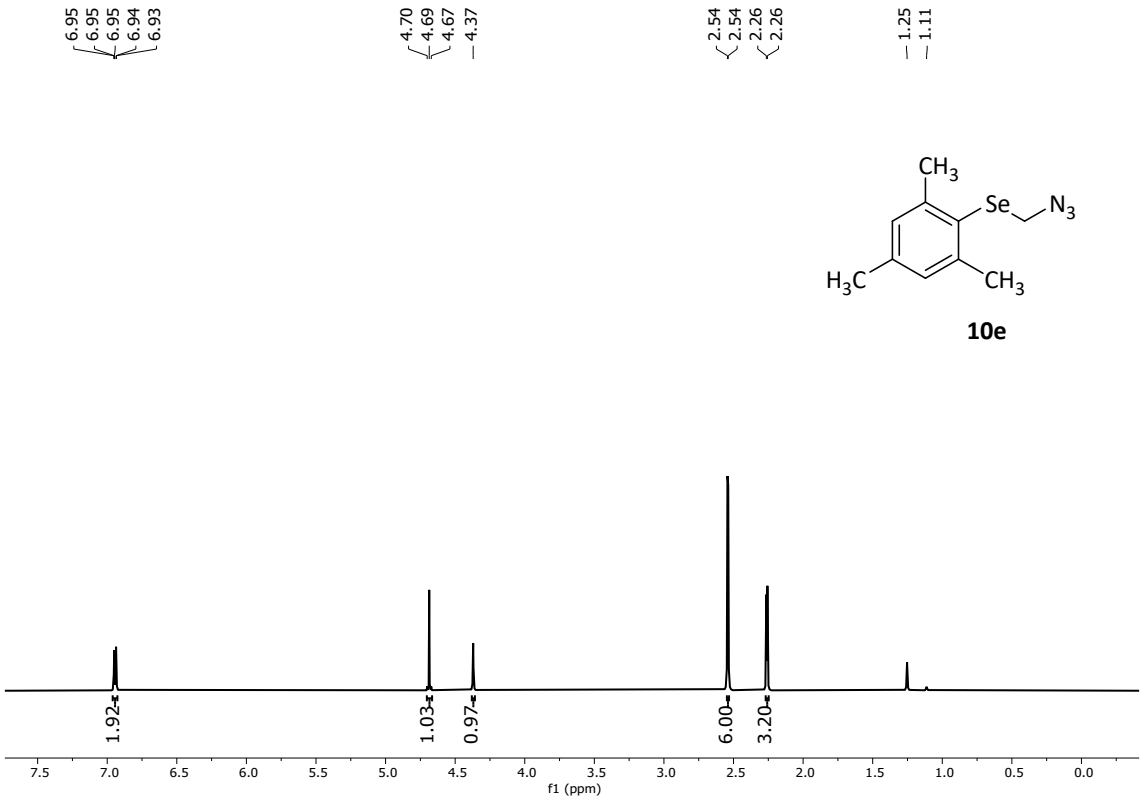

Figure S12. ^{1}H NMR spectrum of compound **10e** in $CDCl_3$ at 500 MHz.

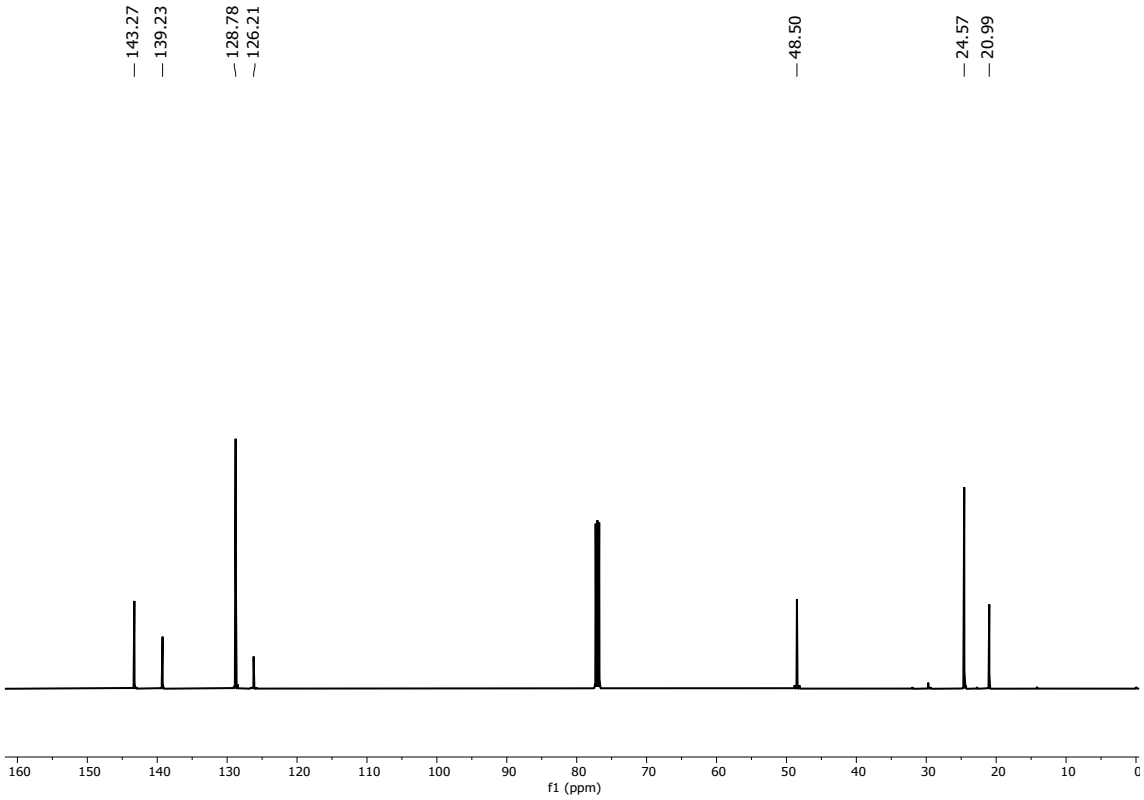

Figure S13. ^{13}C NMR spectrum of compound **10e** in $CDCl_3$ at 125 MHz.

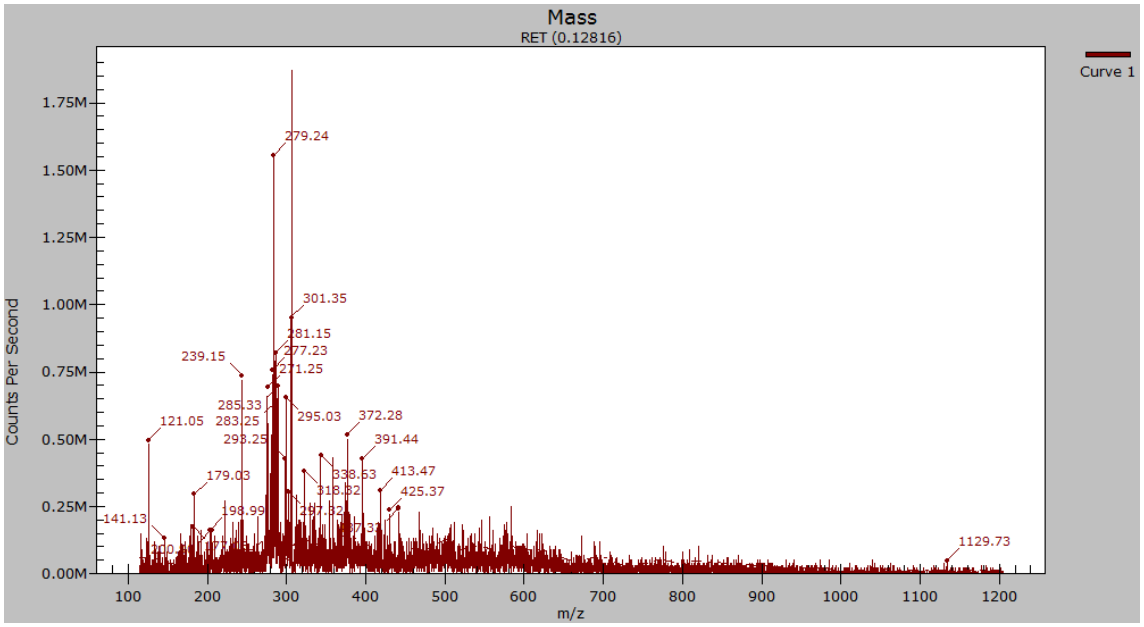

Figure S14. ESI MS spectrum of **10e**.

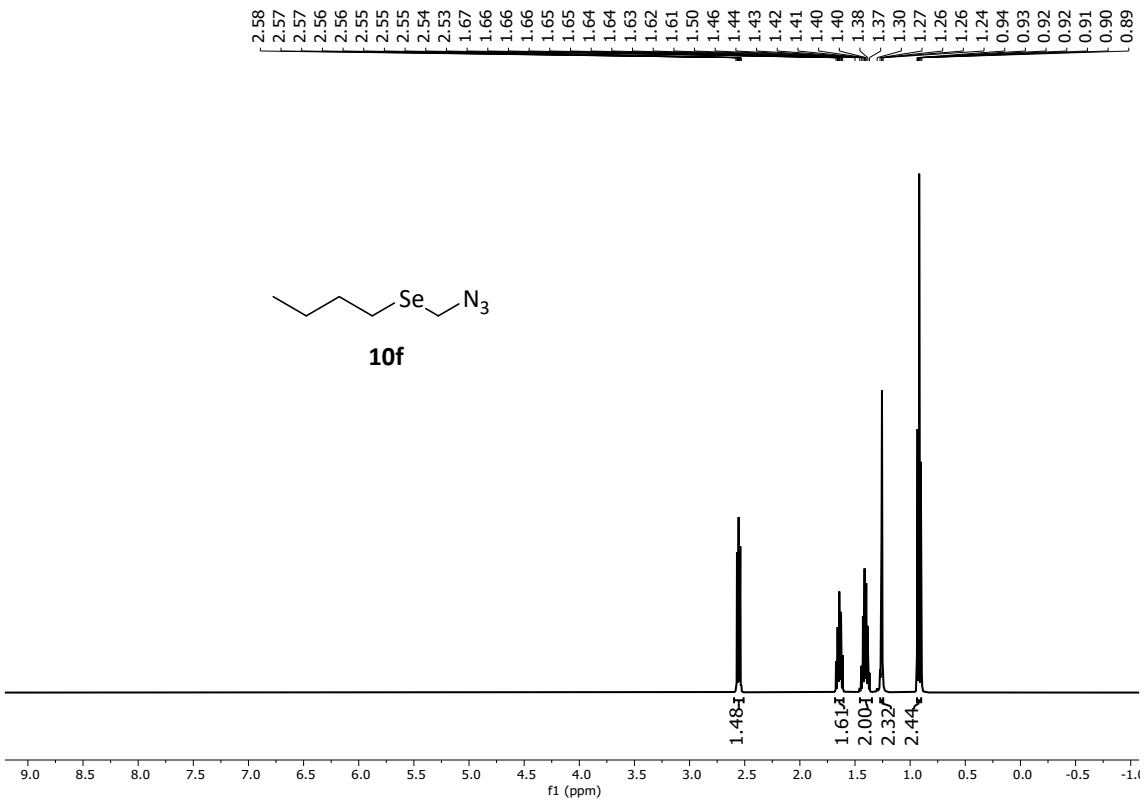

Figure S15. ^{1}H NMR spectrum of compound **10f** in $CDCl_3$ at 500 MHz.

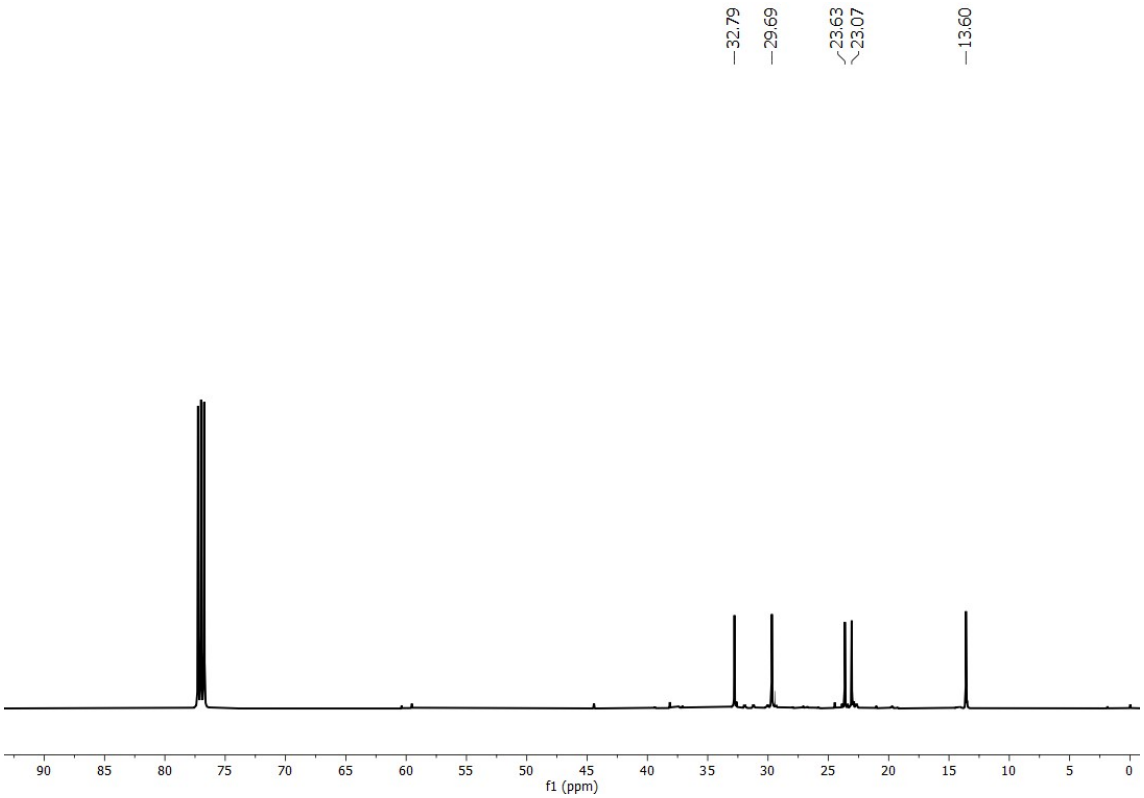

Figure S16. ^{13}C NMR spectrum of compound **10f** in $CDCl_3$ at 125 MHz.

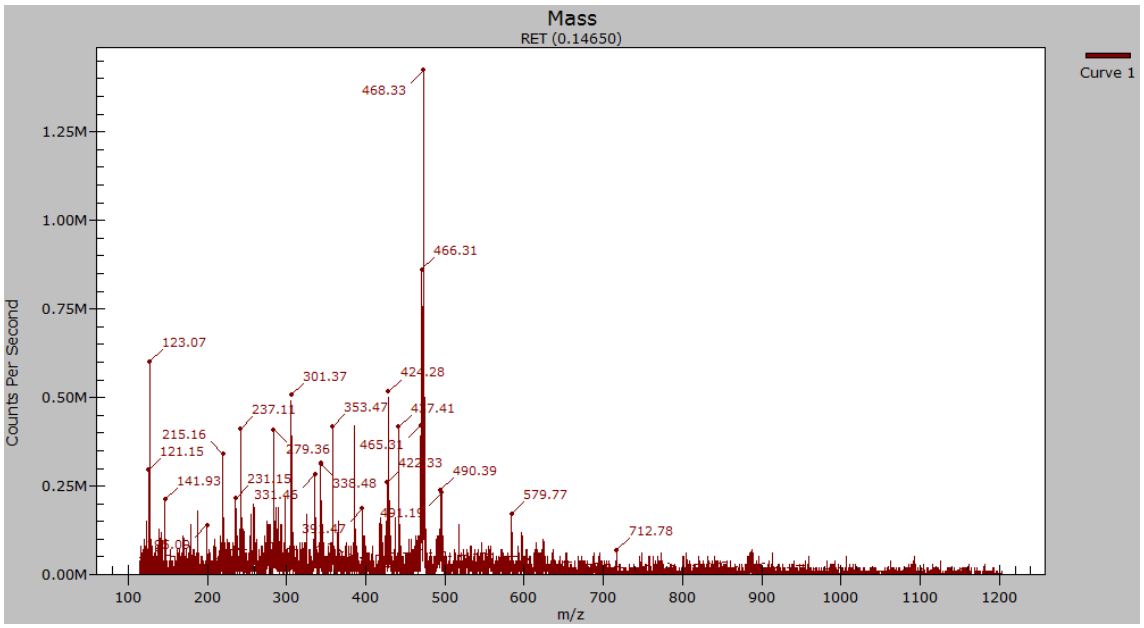

Figure S17. ESI MS spectrum of **10f**.

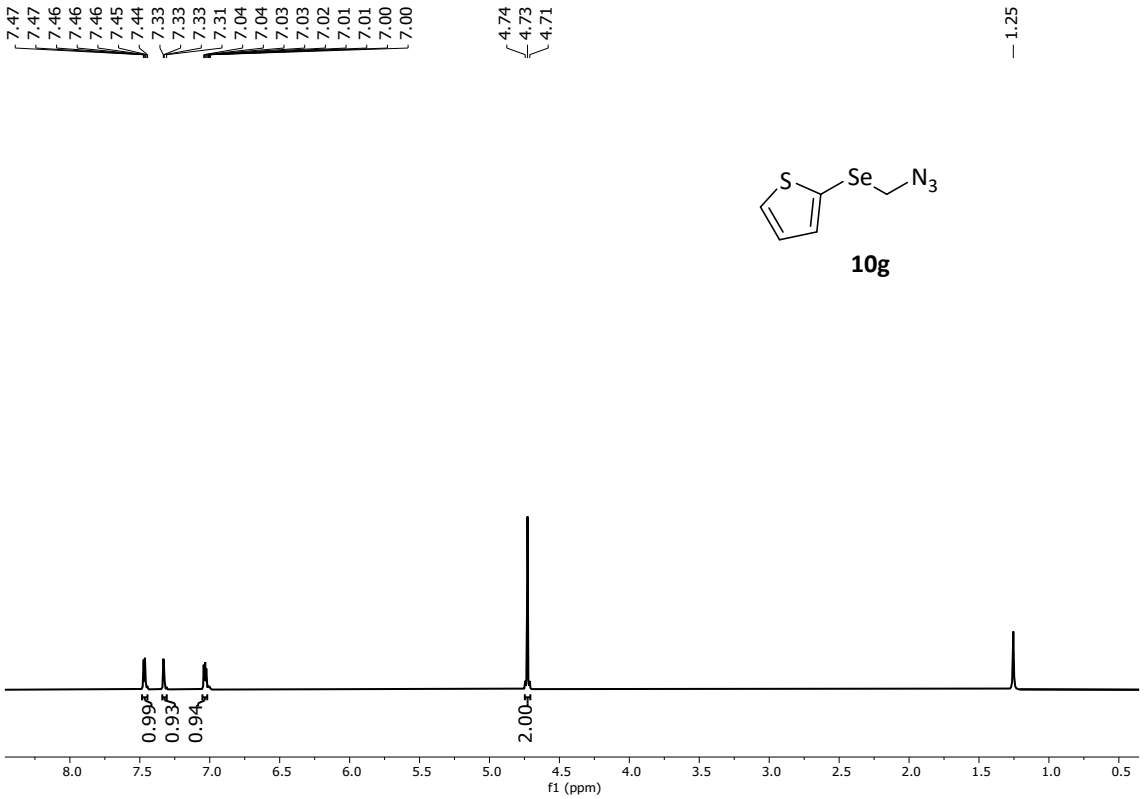

Figure S18. ^{1}H NMR spectrum of compound **10g** in $CDCl_3$ at 500 MHz.

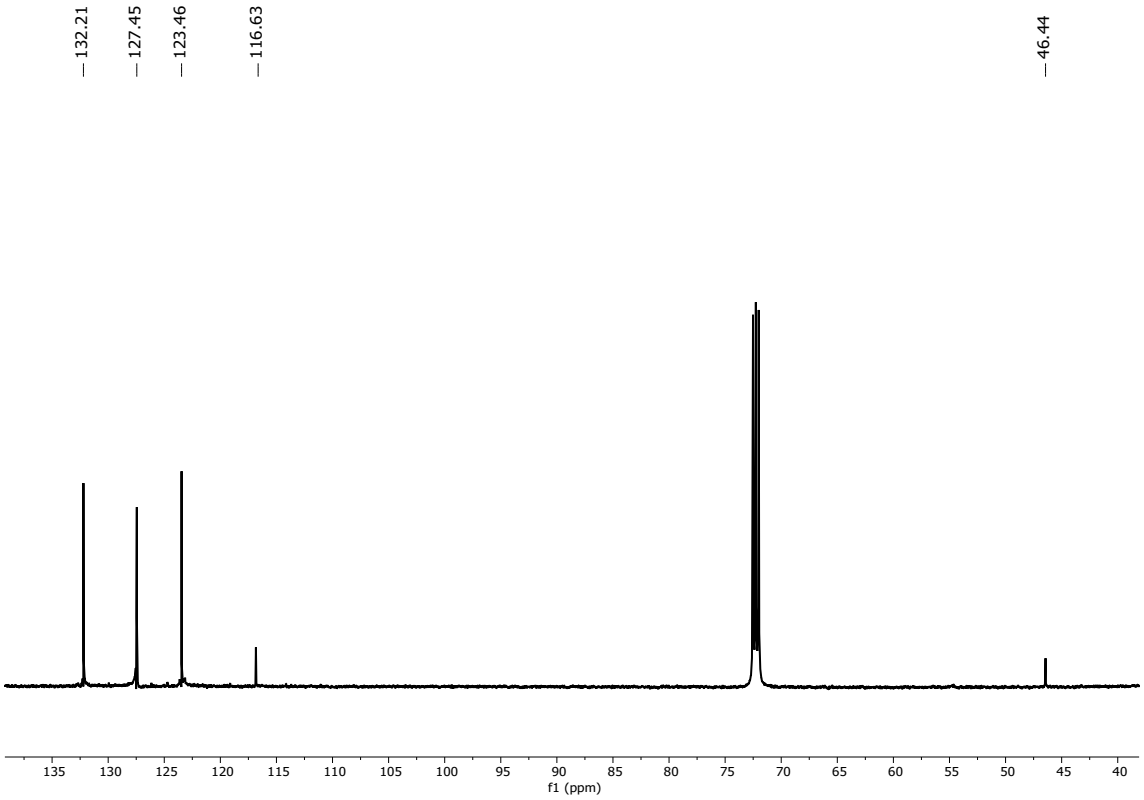

Figure S19. ^{13}C NMR spectrum of compound **10g** in $CDCl_3$ at 125 MHz.

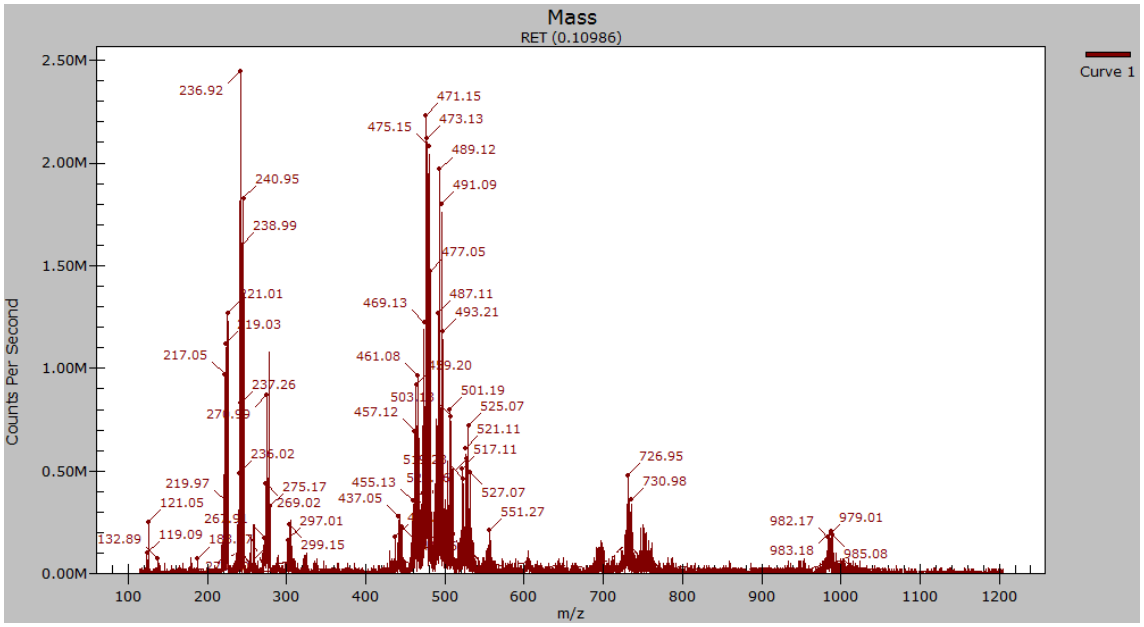

Figure S20. ESI MS spectrum of **10g**.

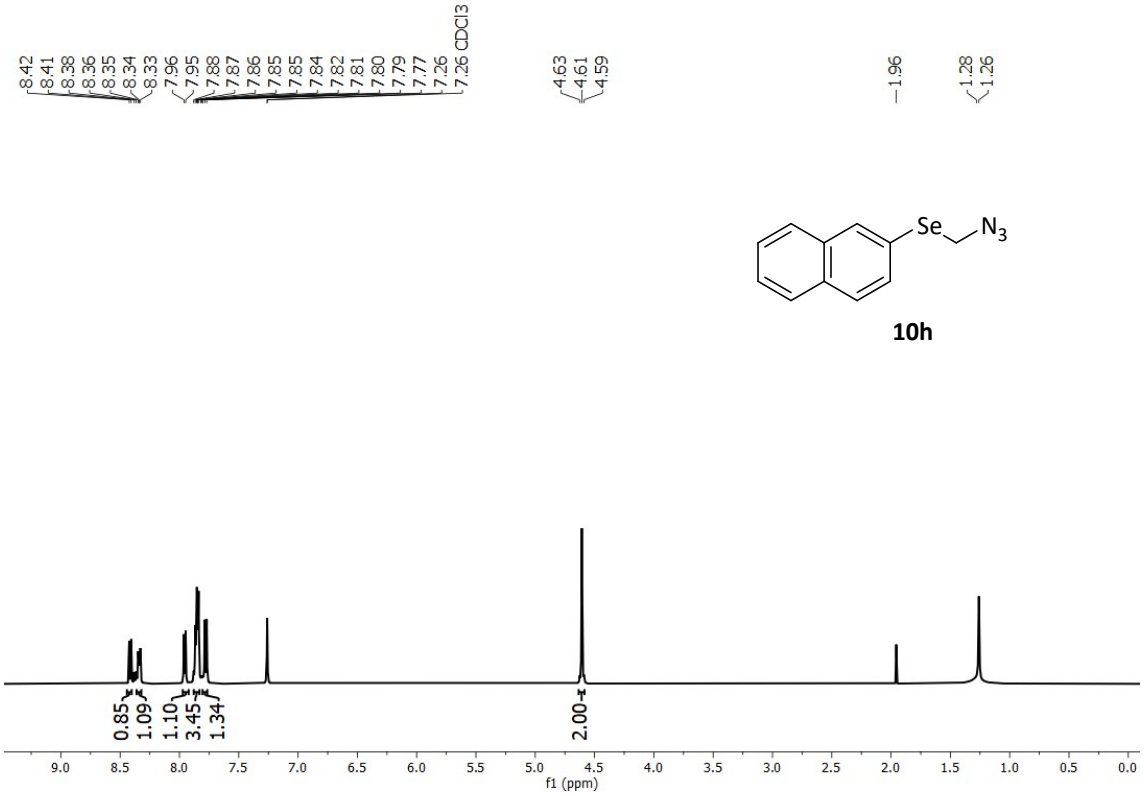

Figure S21. ^{1}H NMR spectrum of compound **10h** in $CDCl_3$ at 500 MHz.

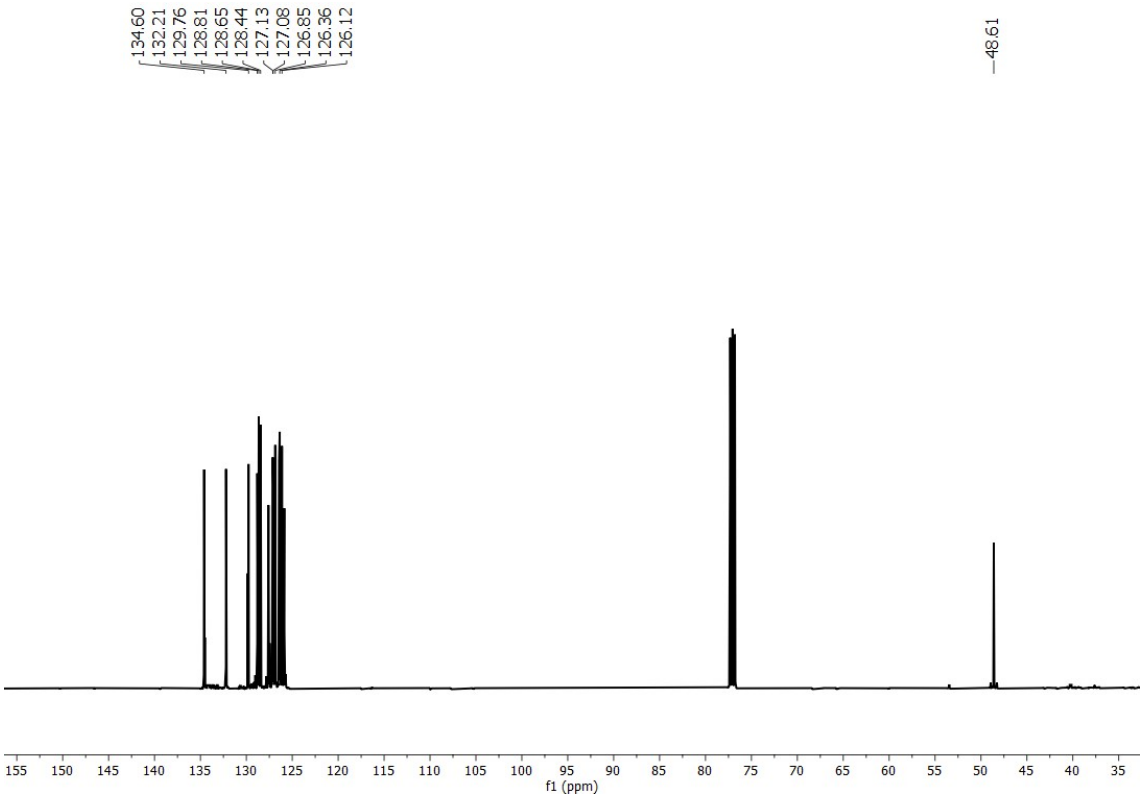

Figure S22. ^{13}C NMR spectrum of compound **10h** in $CDCl_3$ at 125 MHz.

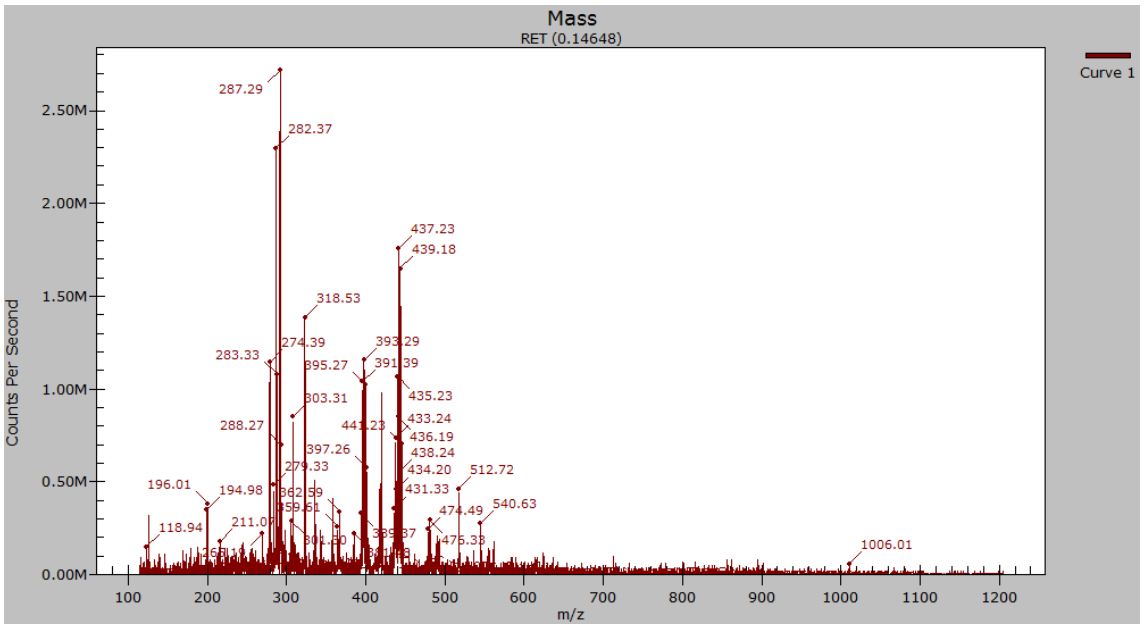

Figure S23. ESI MS spectrum of **10h**.

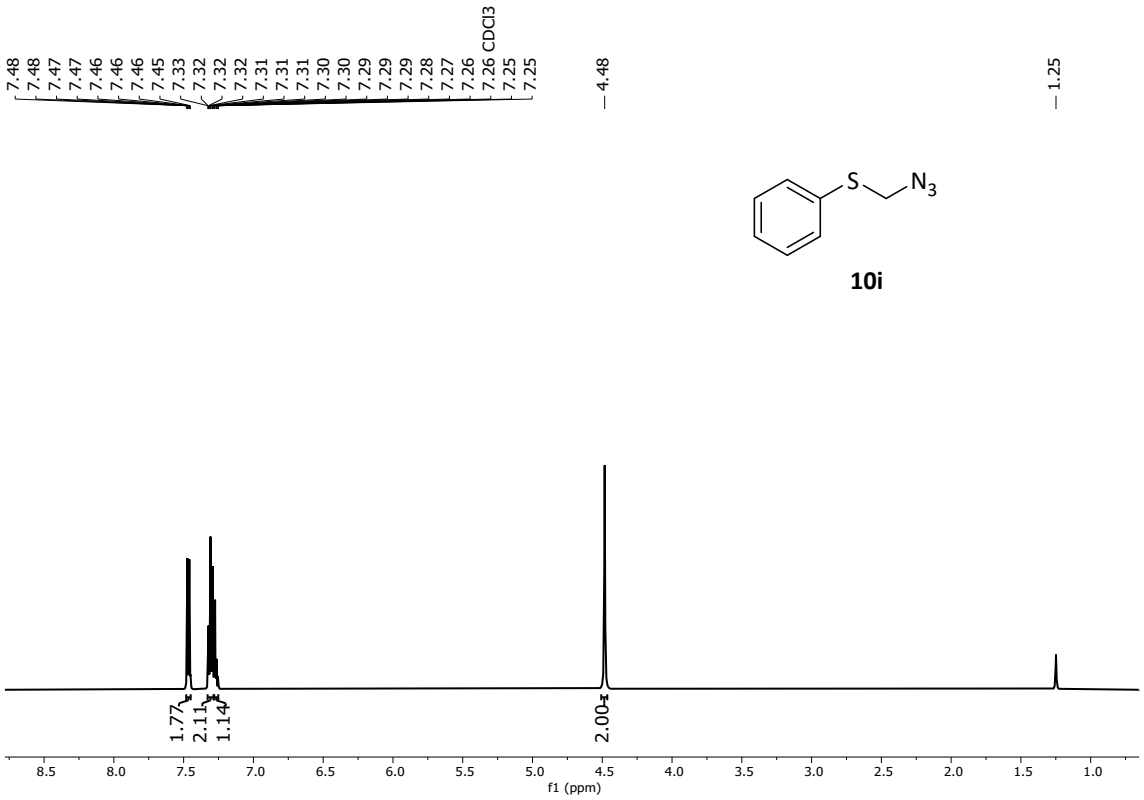

Figure S24. ^{1}H NMR spectrum of compound **10i** in $CDCl_3$ at 500 MHz.

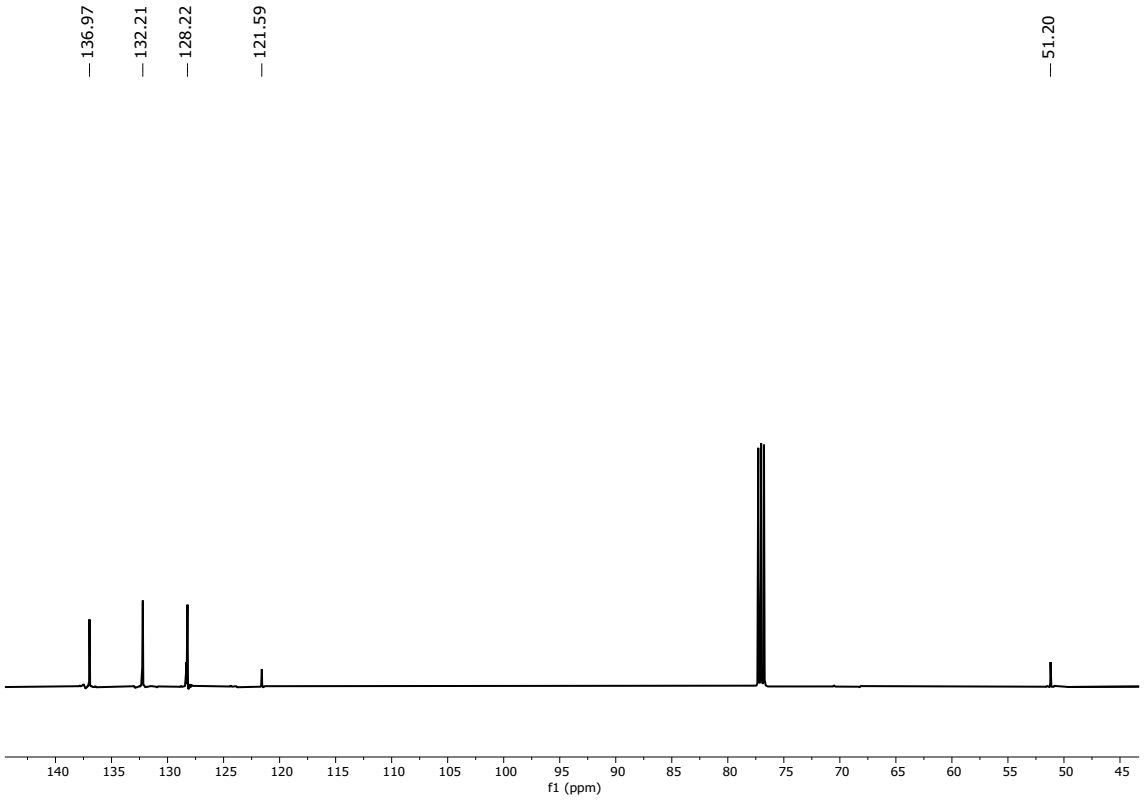

Figure S25. ^{13}C NMR spectrum of compound **10i** in $CDCl_3$ at 125 MHz.

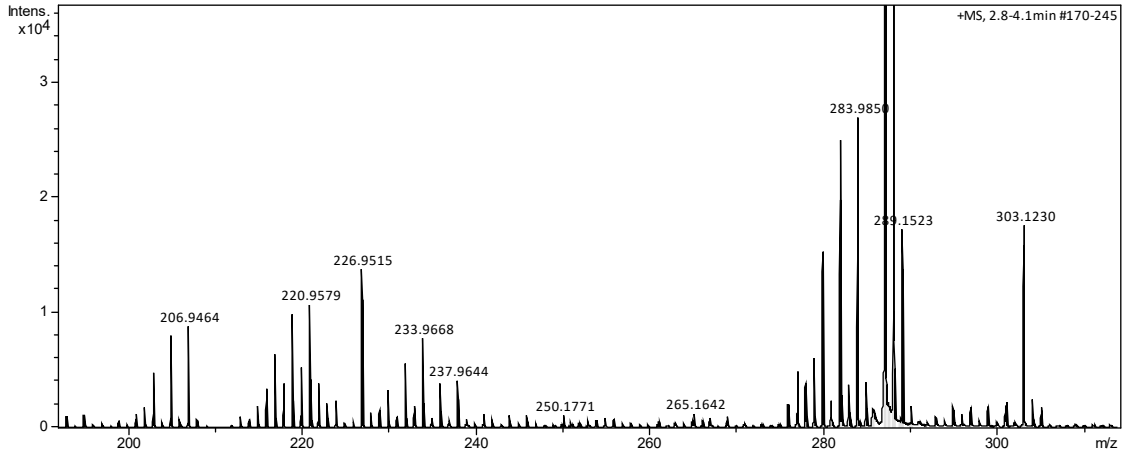

Figure S26. ESI MS spectrum of **10i**.

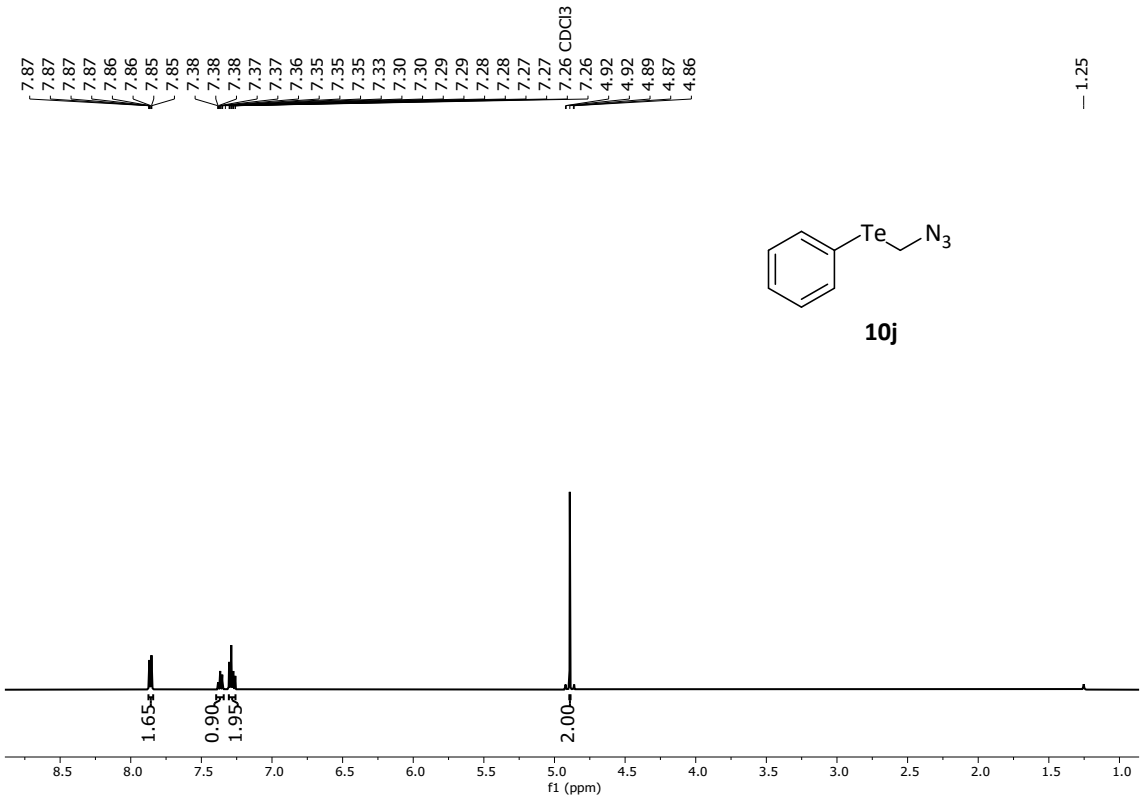

Figure S27. ^{1}H NMR spectrum of compound **10j** in $CDCl_3$ at 500 MHz.

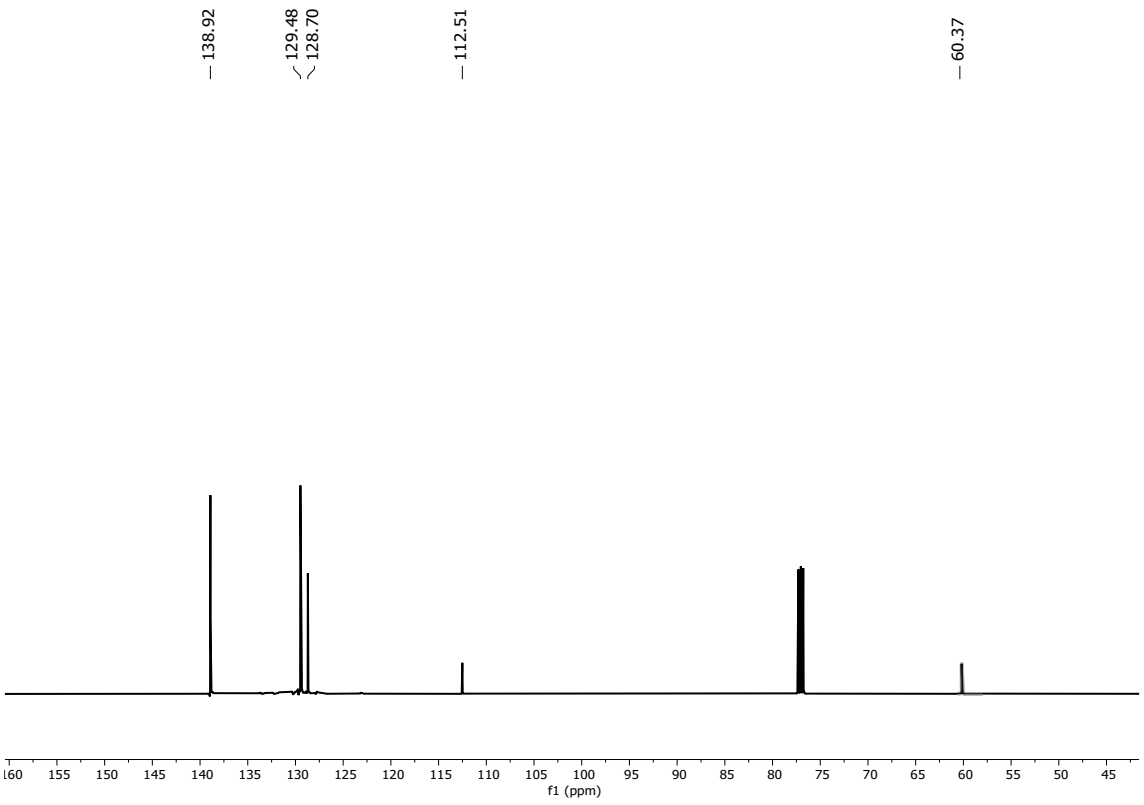

Figure S28. ^{13}C NMR spectrum of compound **10j** in $CDCl_3$ at 125 MHz.

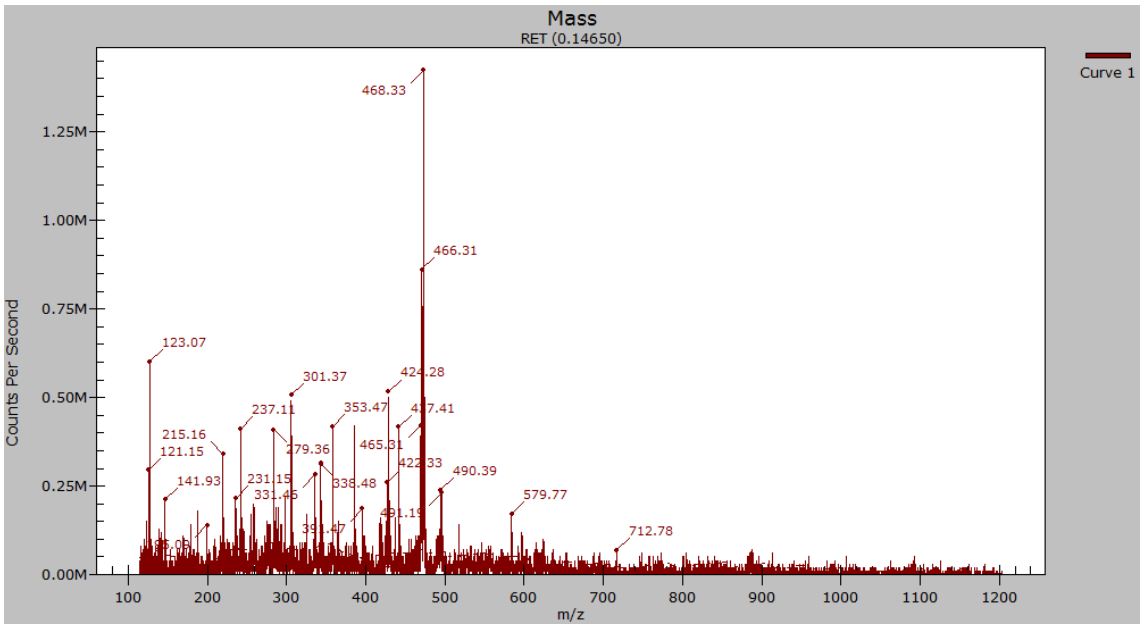

Figure S29. ESI MS spectrum of **10j**.

Structural characterization explained for compound 11a

The singlet at 7.64 ppm was attributed to the triazole aromatic ring's single hydrogen. Finally, because there are no neighboring hydrogens to couple with, the singlet at 5.70 ppm was assigned to the two CH_2-type hydrogens attached to the selenium-containing moiety, and the singlet at 5.21 ppm was assigned to lawsone. In the ^{13}C NMR spectrum, three new signals can be observed: one referring to the 1,2,3-triazole nucleus (C-2' carbon) and the non-hydrogenated carbon of the triazole linked to propargylated lawsone at 141.9 ppm, another signal referring to the triazole hydrogenated carbon (C-3') at 123.6 ppm, and the last one referring to the carbon linked to the organoselenium fraction (C-4') at 44.7 ppm

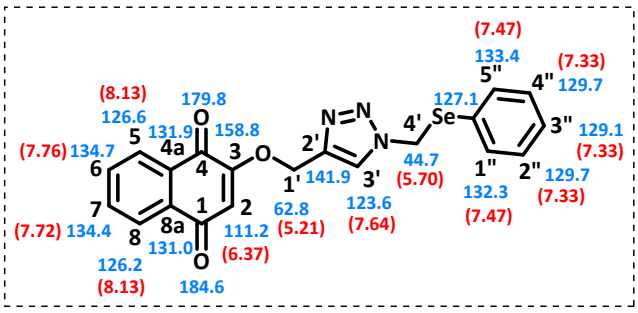

Figure S30. Atom numbering (in black), ^{1}H- (in red) and ^{13}C- (in blue) NMR chemical shifts for compound **11a** (average data).

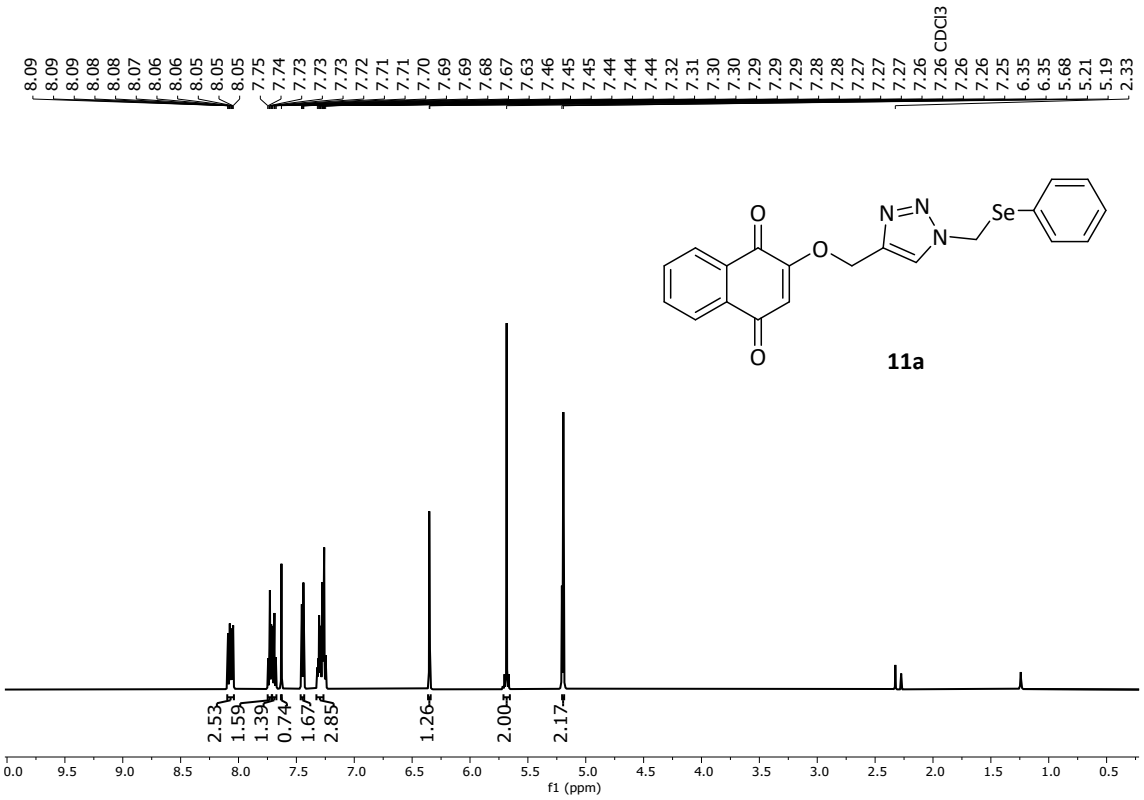

Figure S31. ^{1}H NMR spectrum of compound **11a** in $CDCl_3$ at 500 MHz.

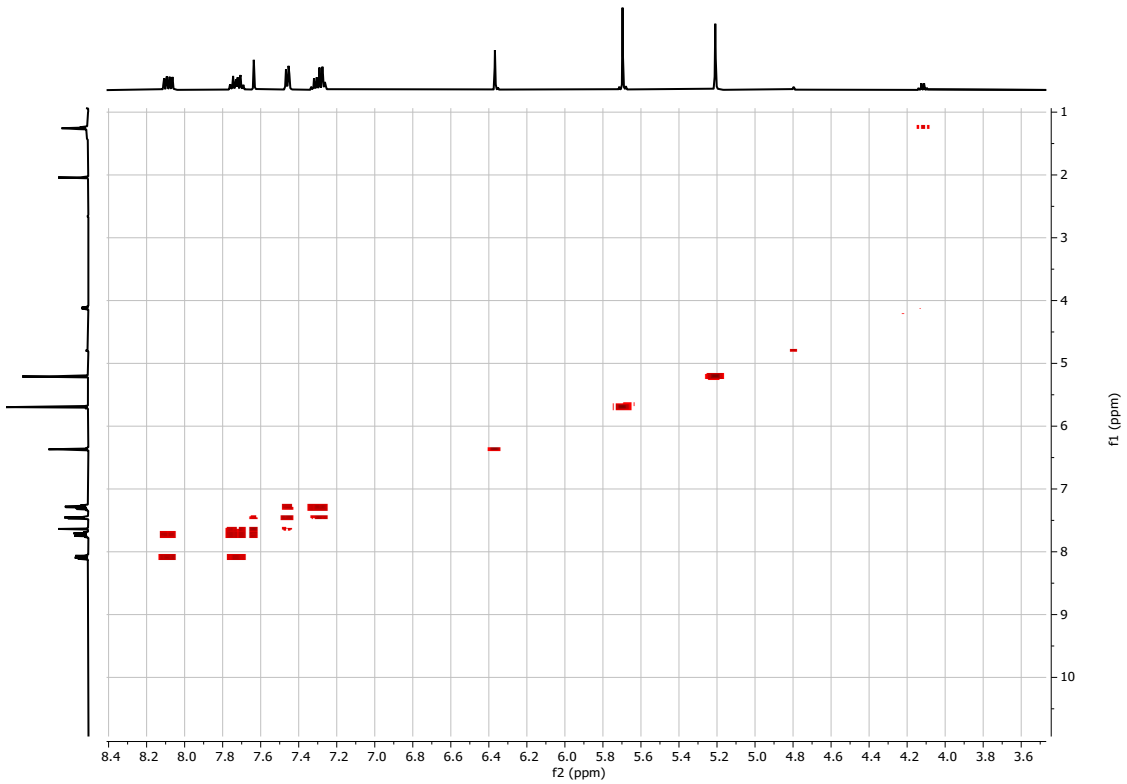

Figure S32. ^{1}H x ^{1}H-COSY spectrum of compound **11a** in $CDCl_3$ at 500 MHz.

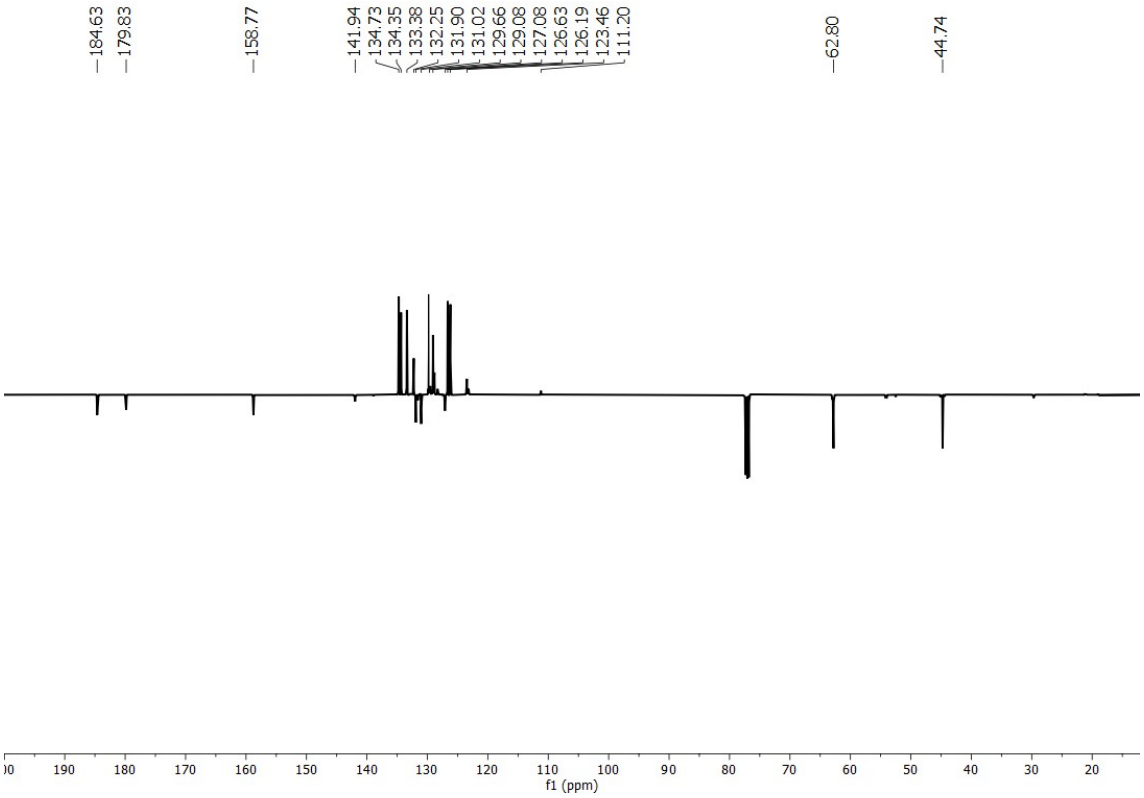

Figure S33. ^{13}C-APT NMR spectrum of compound **11a** in $CDCl_3$ at 125 MHz.

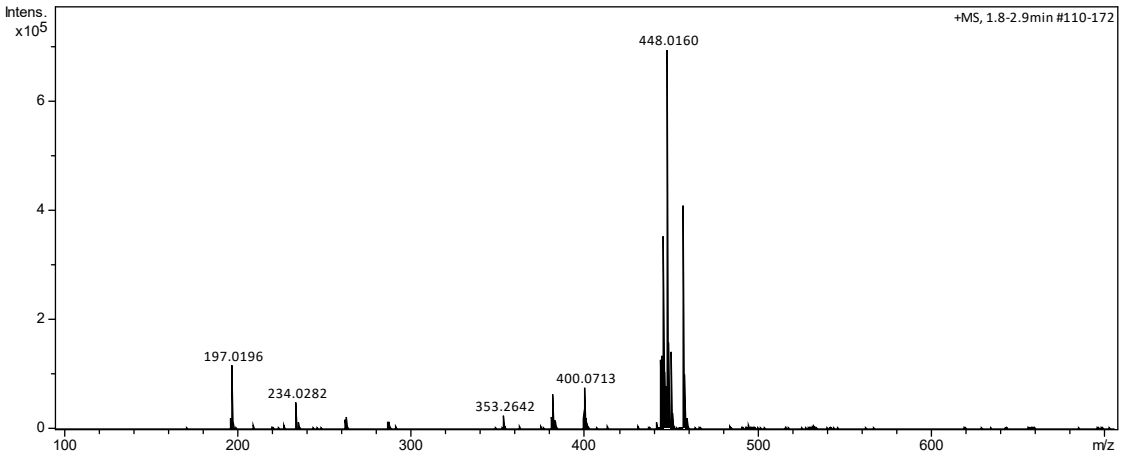

Figure S34. ESI MS spectrum of **11a**.

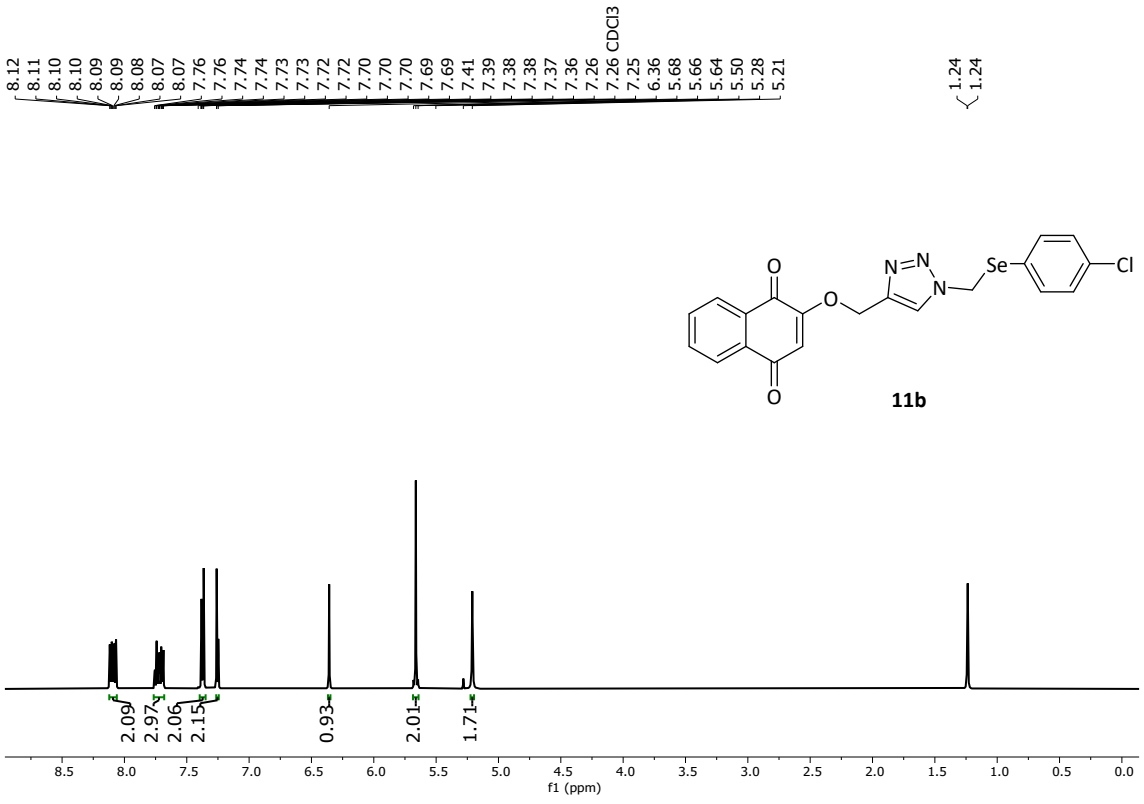

Figure S35. ^{1}H NMR spectrum of compound **11b** in $CDCl_3$ at 500 MHz.

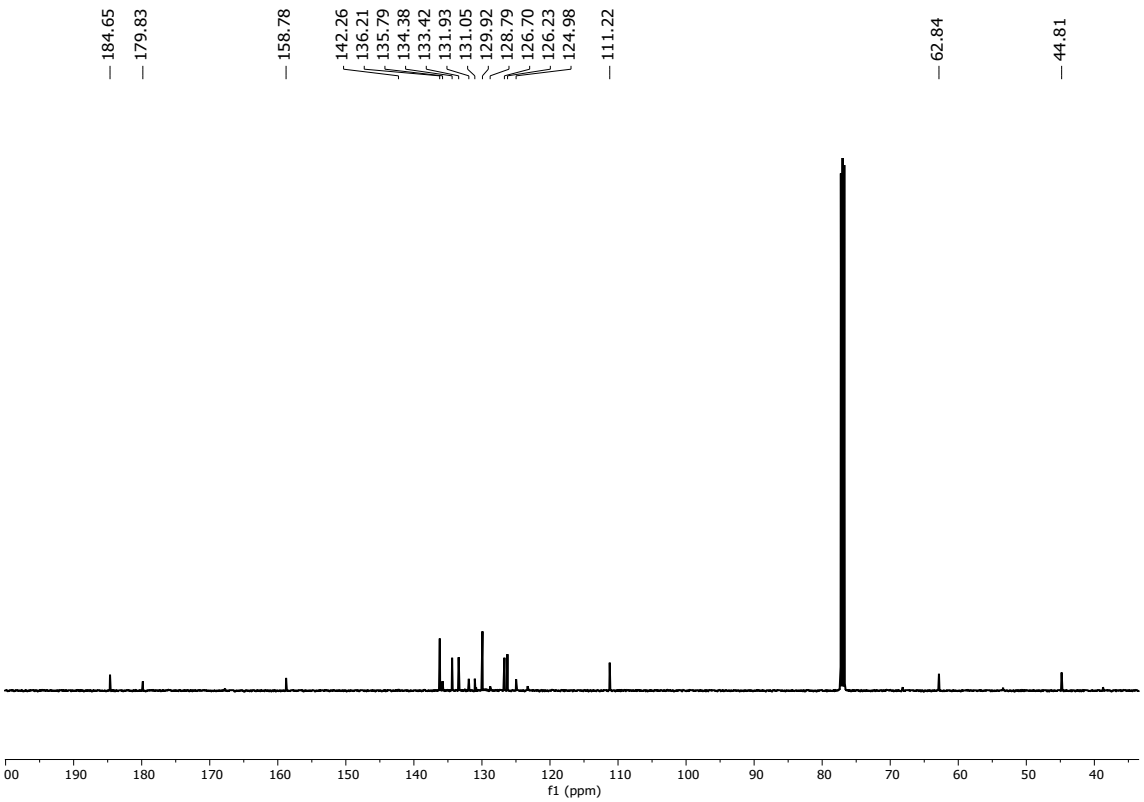

Figure S36. ^{13}C NMR spectrum of compound **11b** in $CDCl_3$ at 125 MHz.

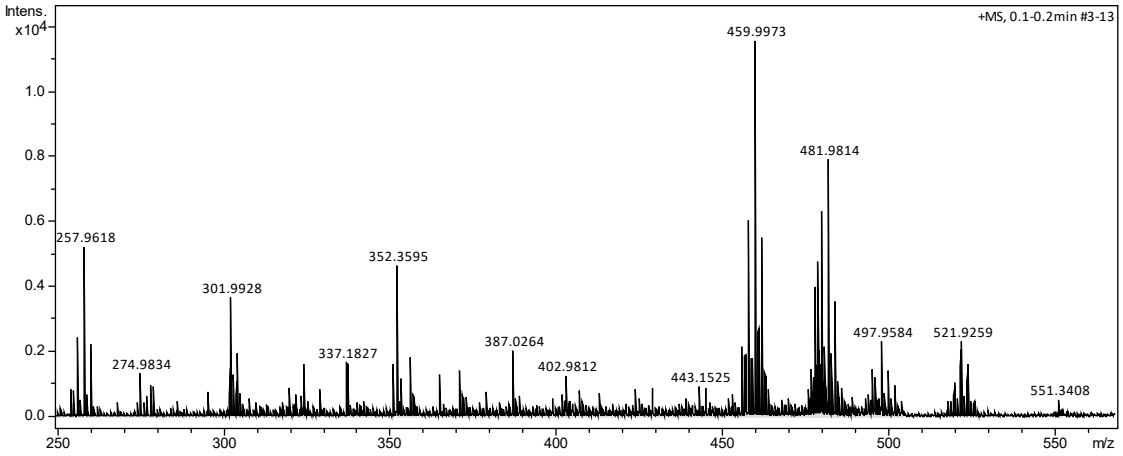

Figure S37. ESI MS spectrum of **11b**.

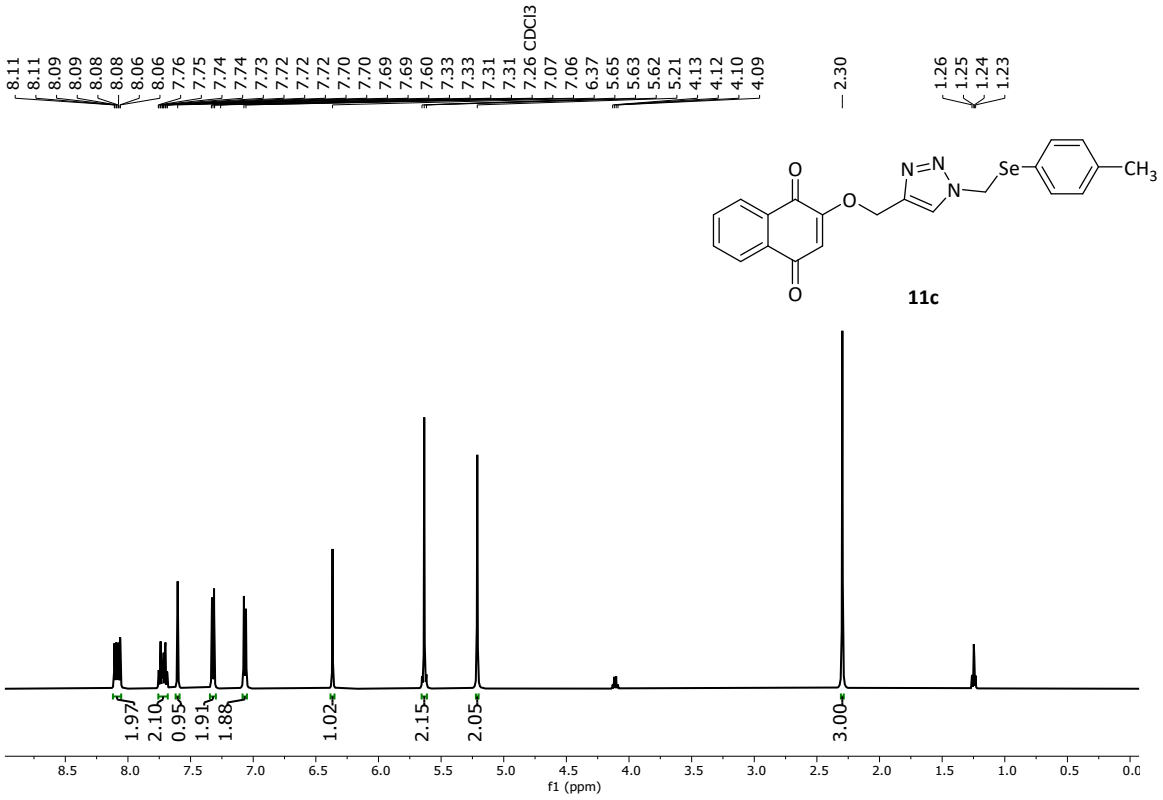

Figure S38. ^{1}H NMR spectrum of compound **11c** in $CDCl_3$ at 500 MHz.

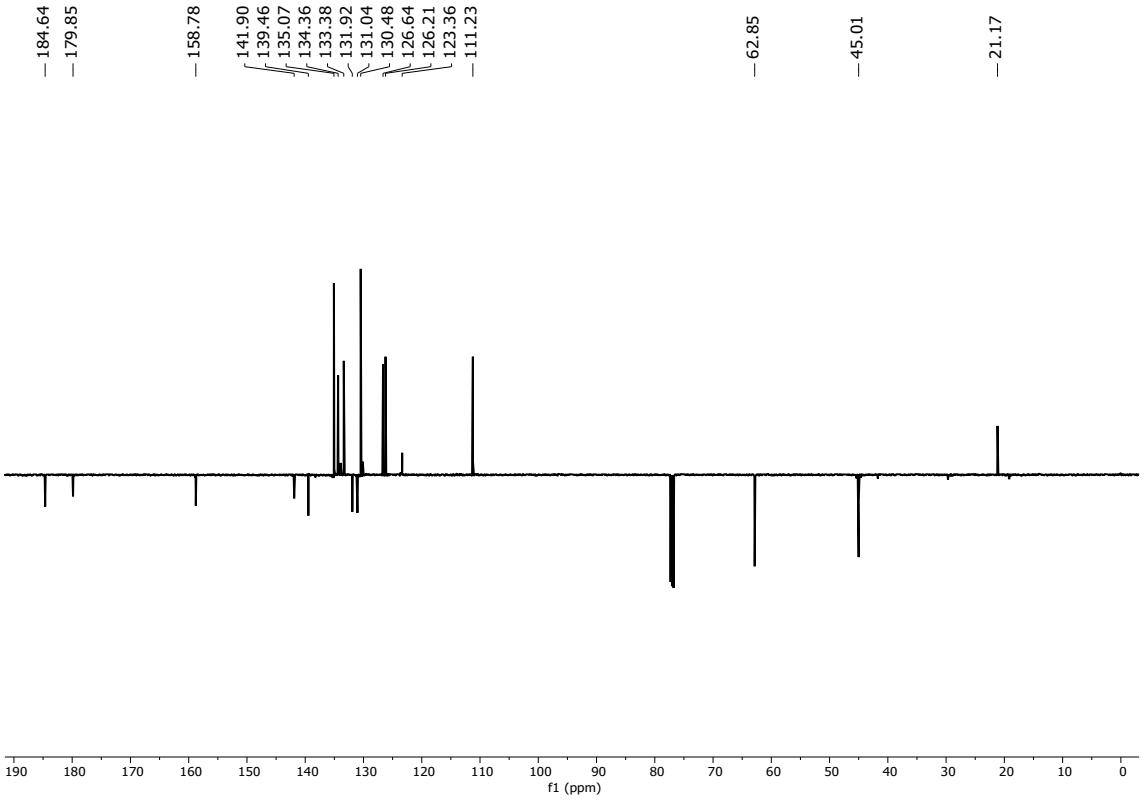

Figure S39. ^{13}C NMR spectrum of compound **11c** in $CDCl_3$ at 125 MHz.

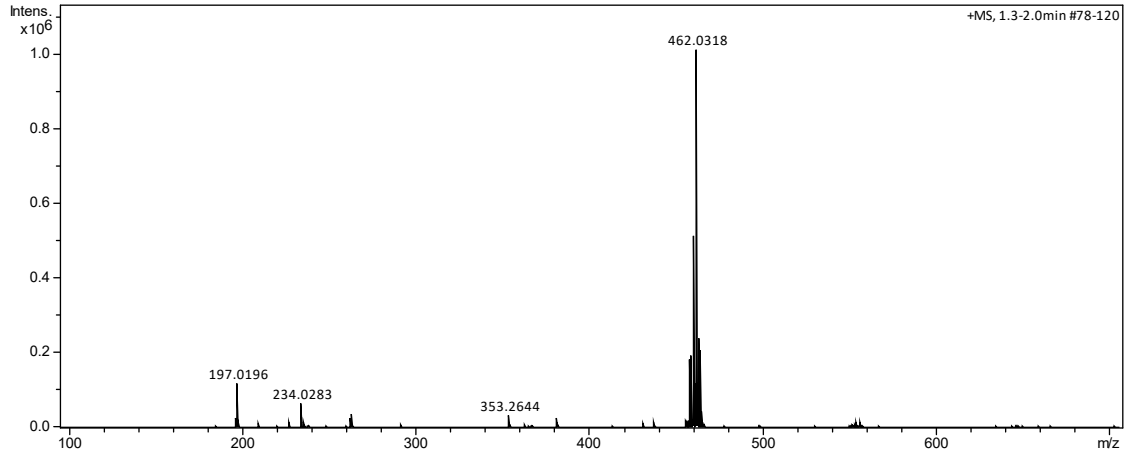

Figure S40. ESI MS spectrum of **11c**.

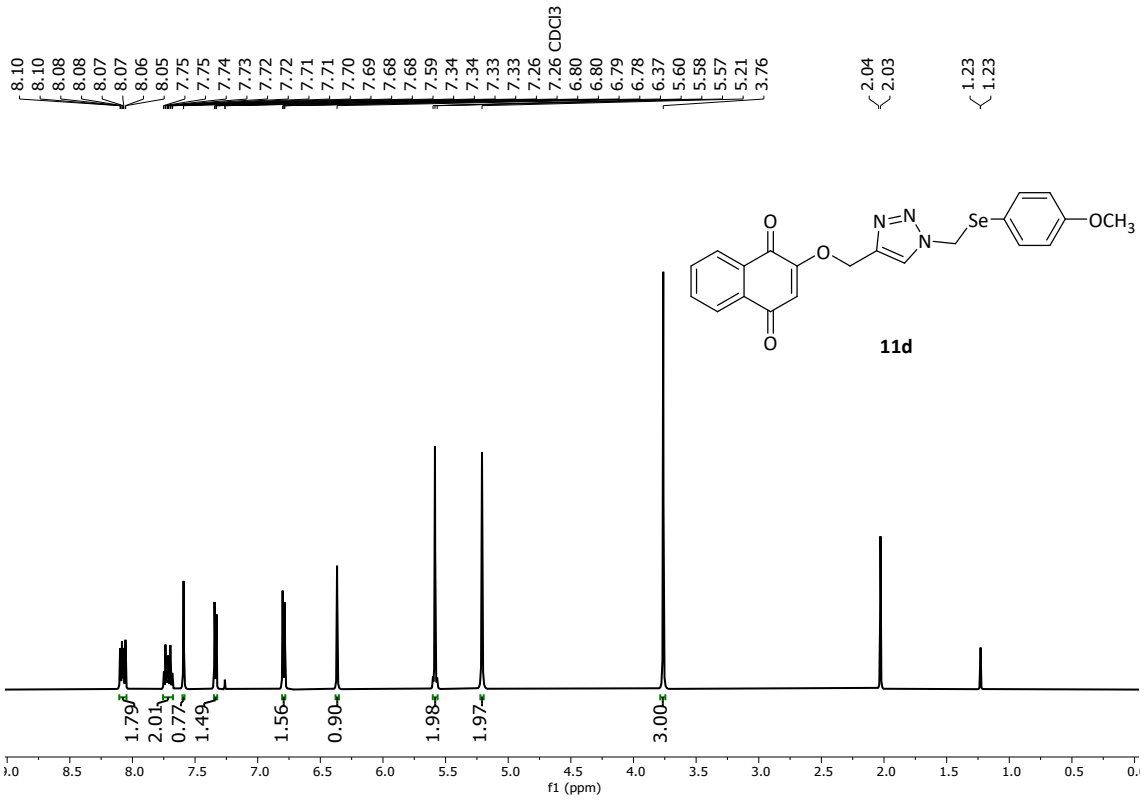

Figure S41. ^{1}H NMR spectrum of compound **11d** in $CDCl_3$ at 500 MHz.

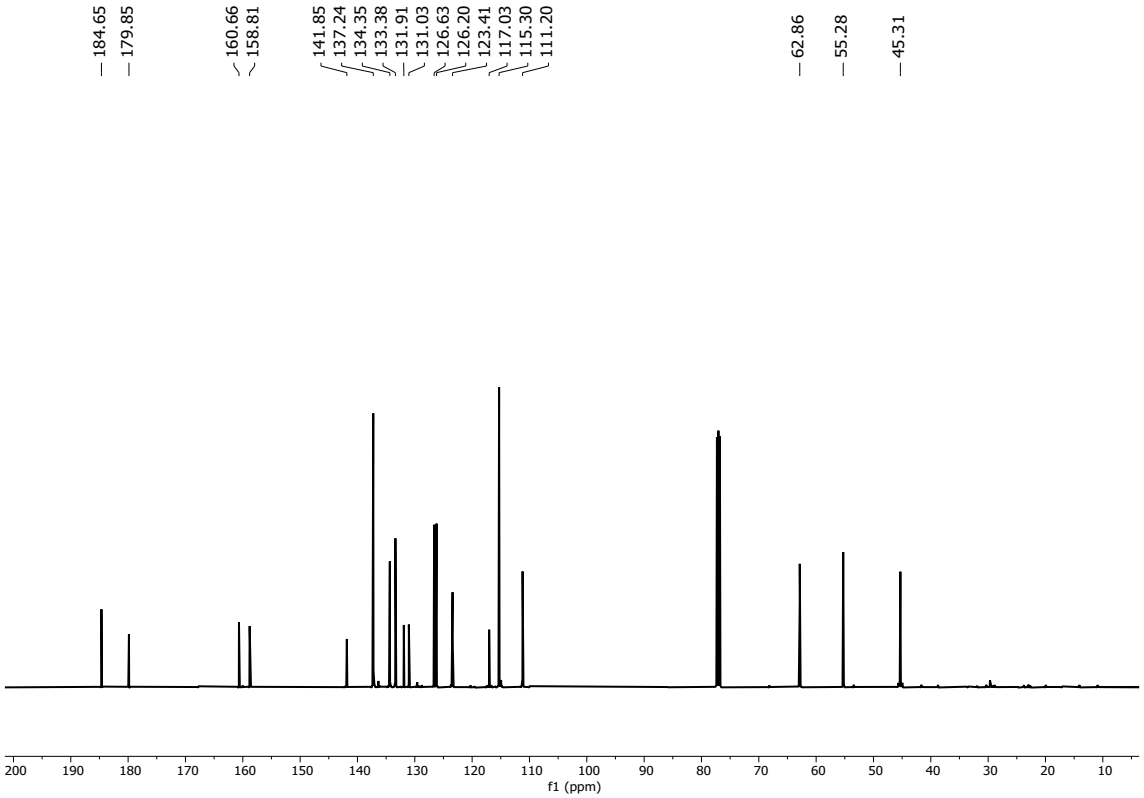

Figure S42. ^{13}C NMR spectrum of compound **11d** in $CDCl_3$ at 125 MHz.

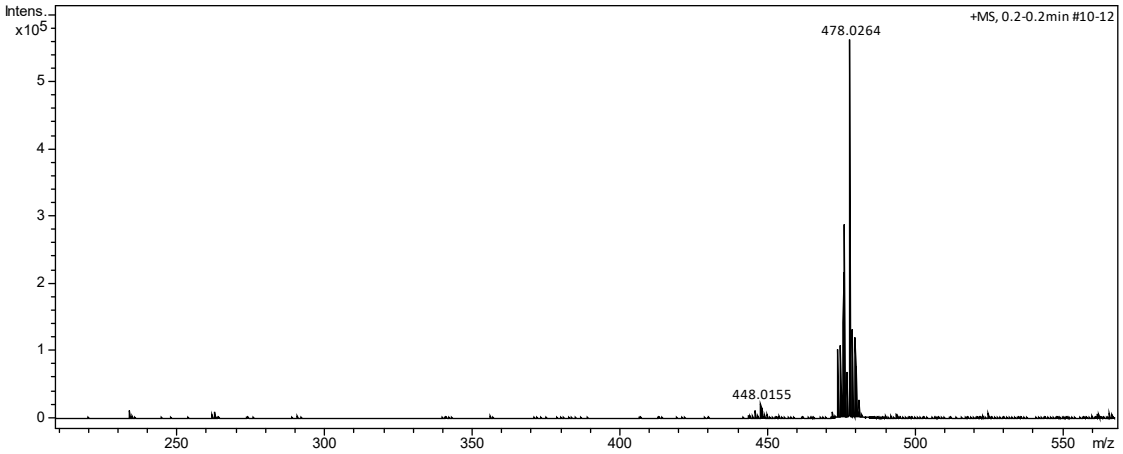

Figure S43. ESI MS spectrum of **11d**.

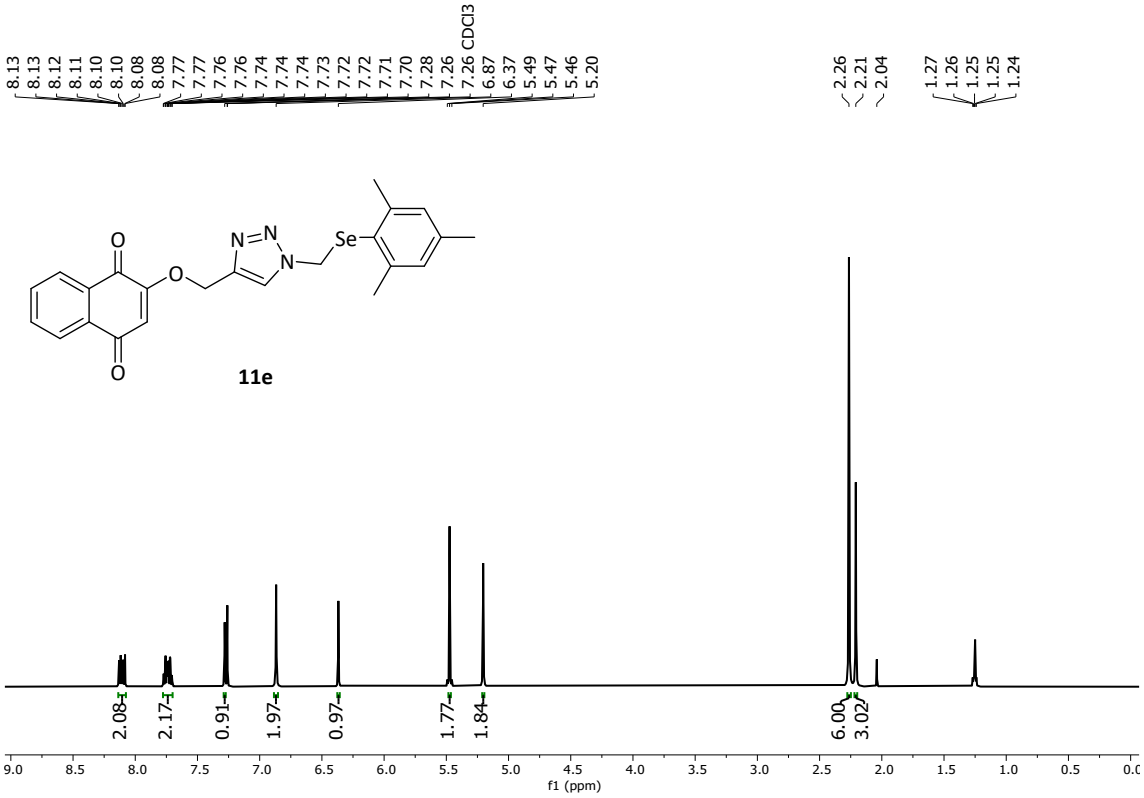

Figure S44. ^{1}H NMR spectrum of compound **11e** in $CDCl_3$ at 500 MHz.

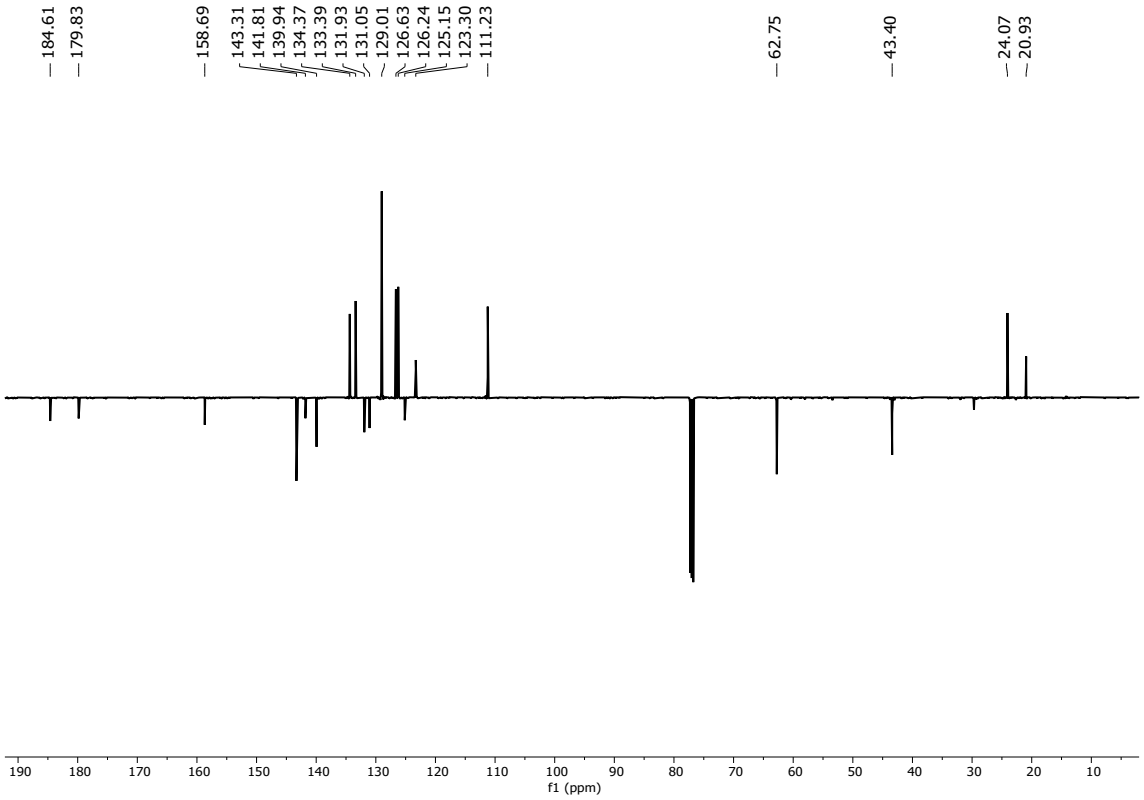

Figure S45. ^{13}C-APT NMR spectrum of compound **11e** in $CDCl_3$ at 125 MHz.

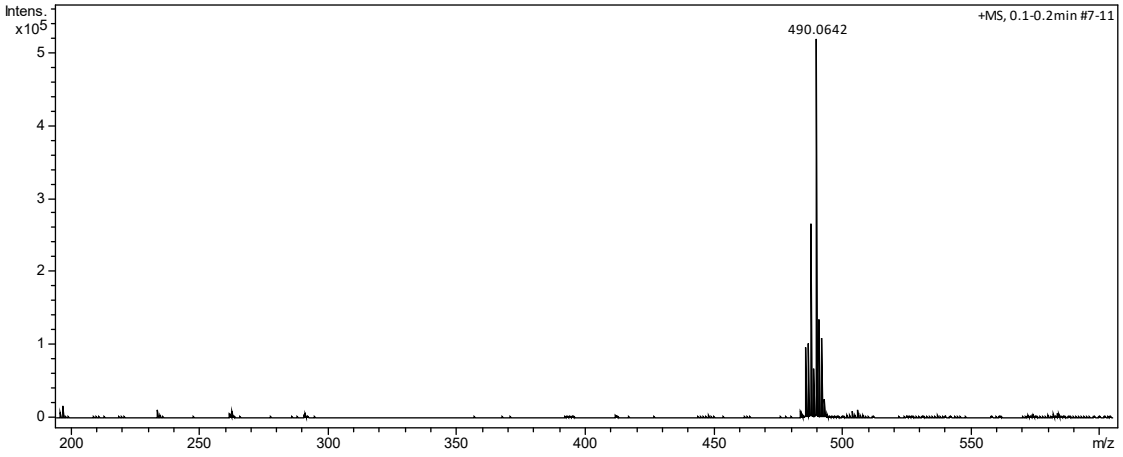

Figure S46. ESI MS spectrum of **11e**.

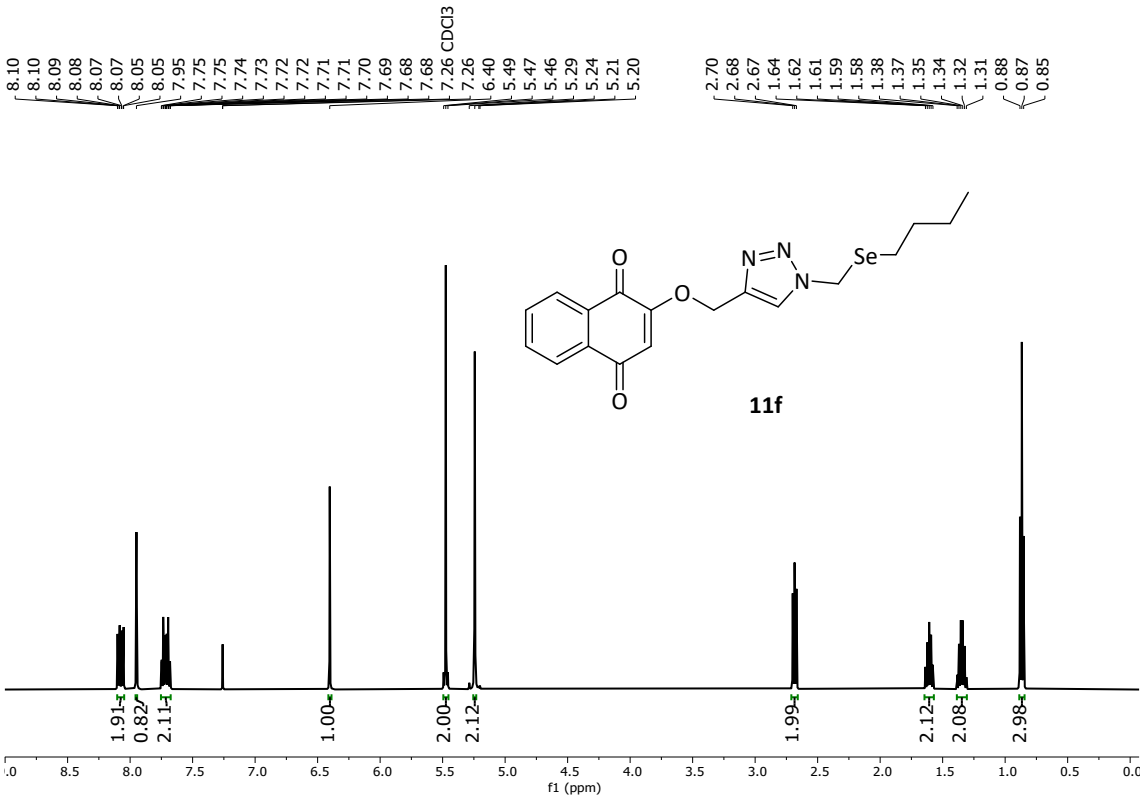

Figure S47. ^{1}H NMR spectrum of compound **11f** in $CDCl_3$ at 500 MHz.

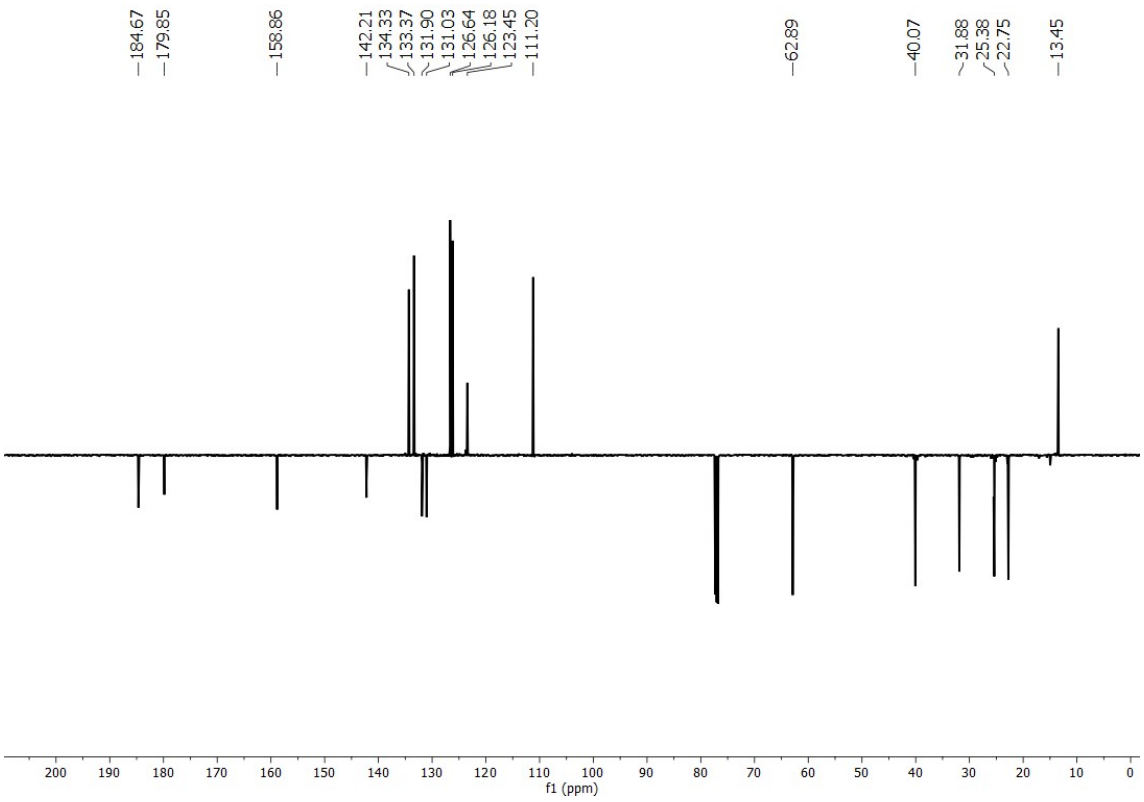

Figure S48. ^{13}C-APT NMR spectrum of compound **11f** in $CDCl_3$ at 125 MHz.

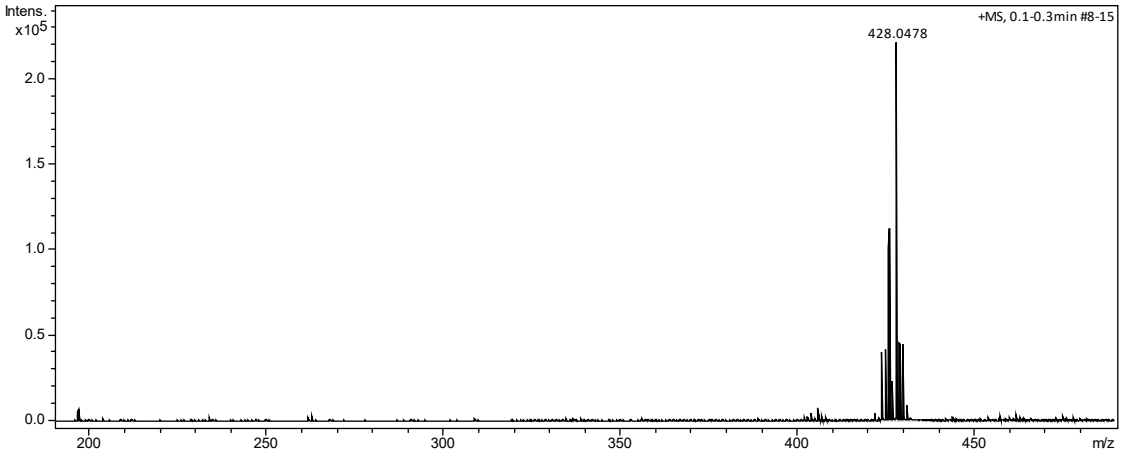

Figure S49. ESI MS spectrum of **11f**.

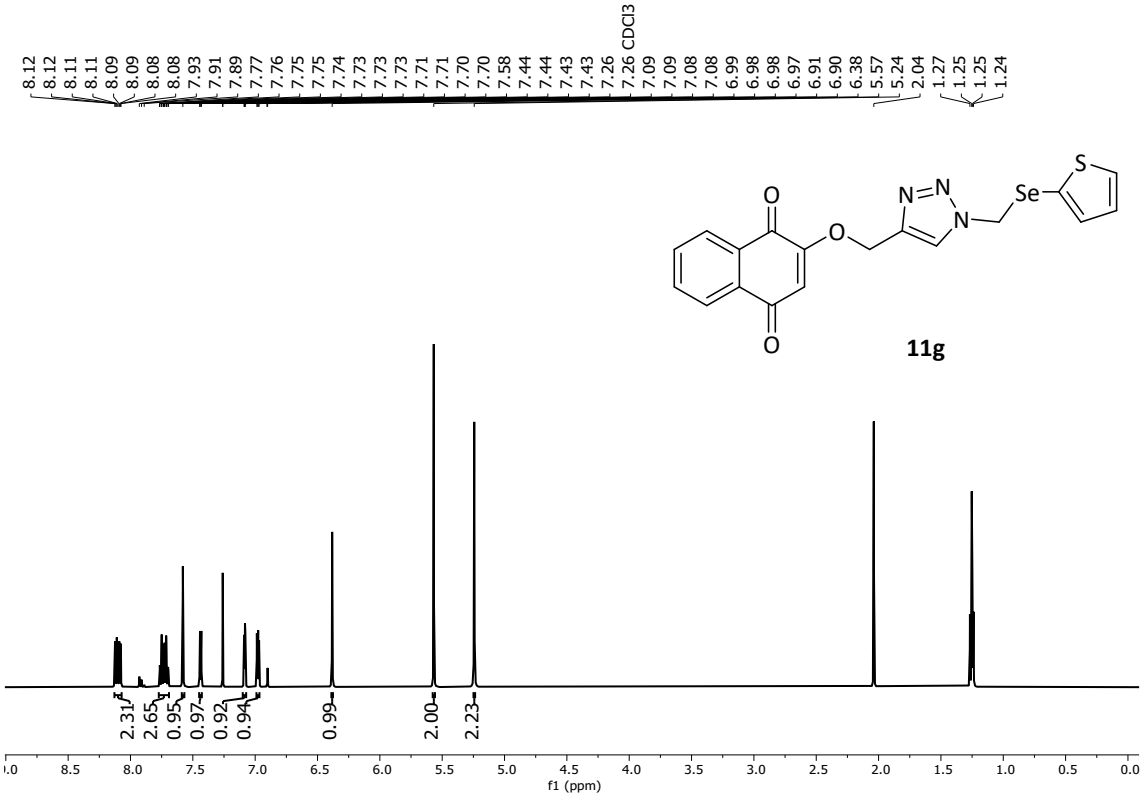

Figure S50. ^{1}H NMR spectrum of compound **11g** in $CDCl_3$ at 500 MHz.

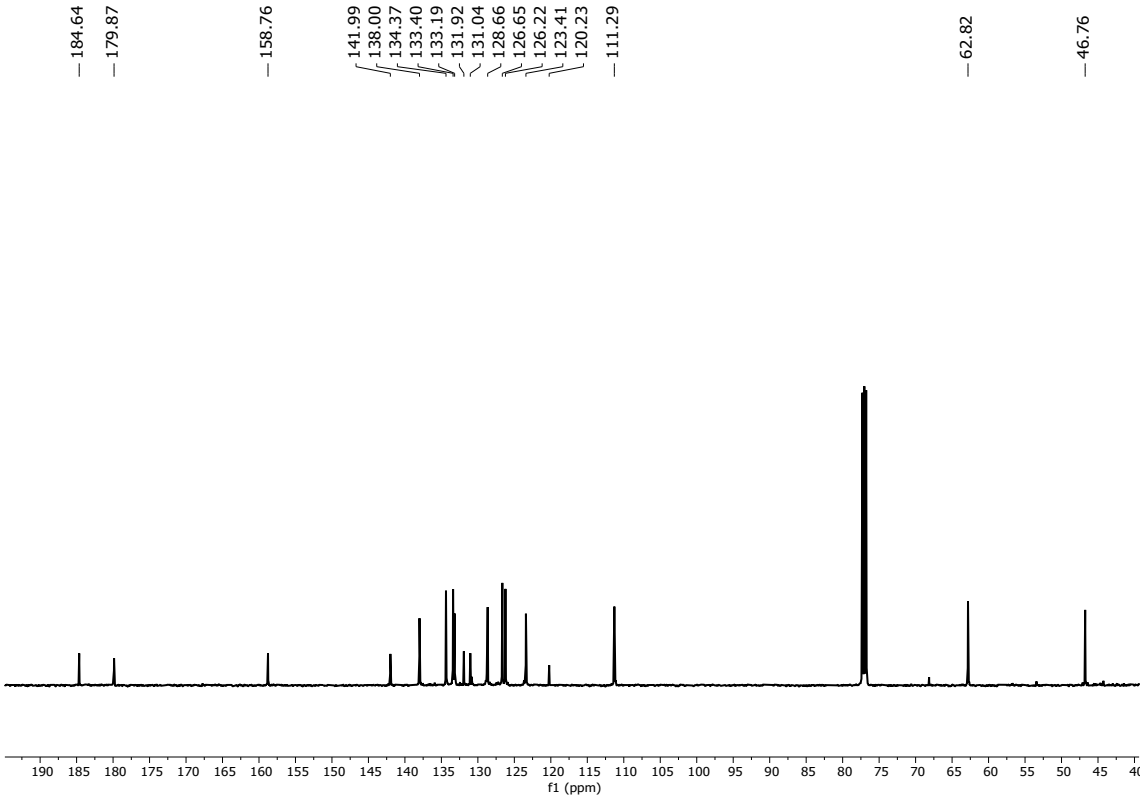

Figure S51. ^{13}C NMR spectrum of compound **11g** in $CDCl_3$ at 125 MHz.

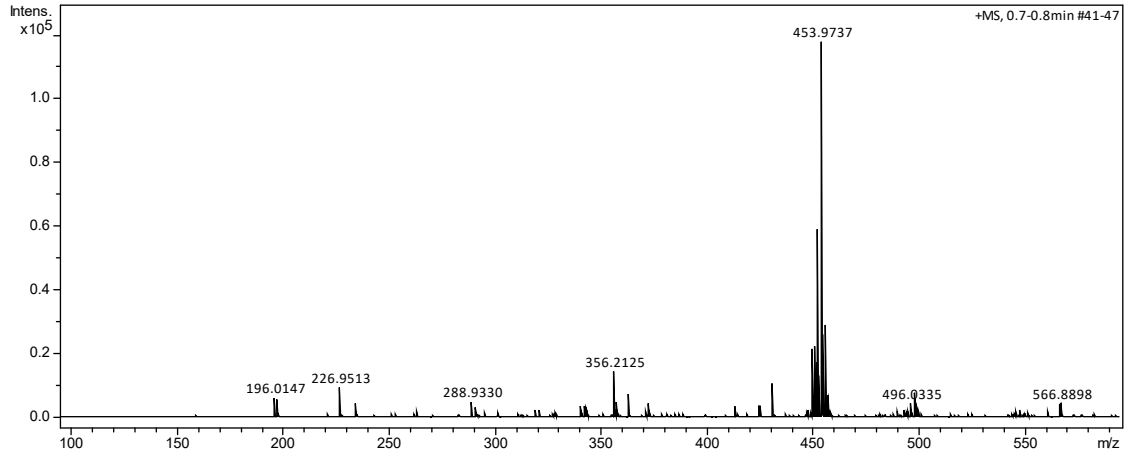

Figure S52. ESI MS spectrum of **11g**.

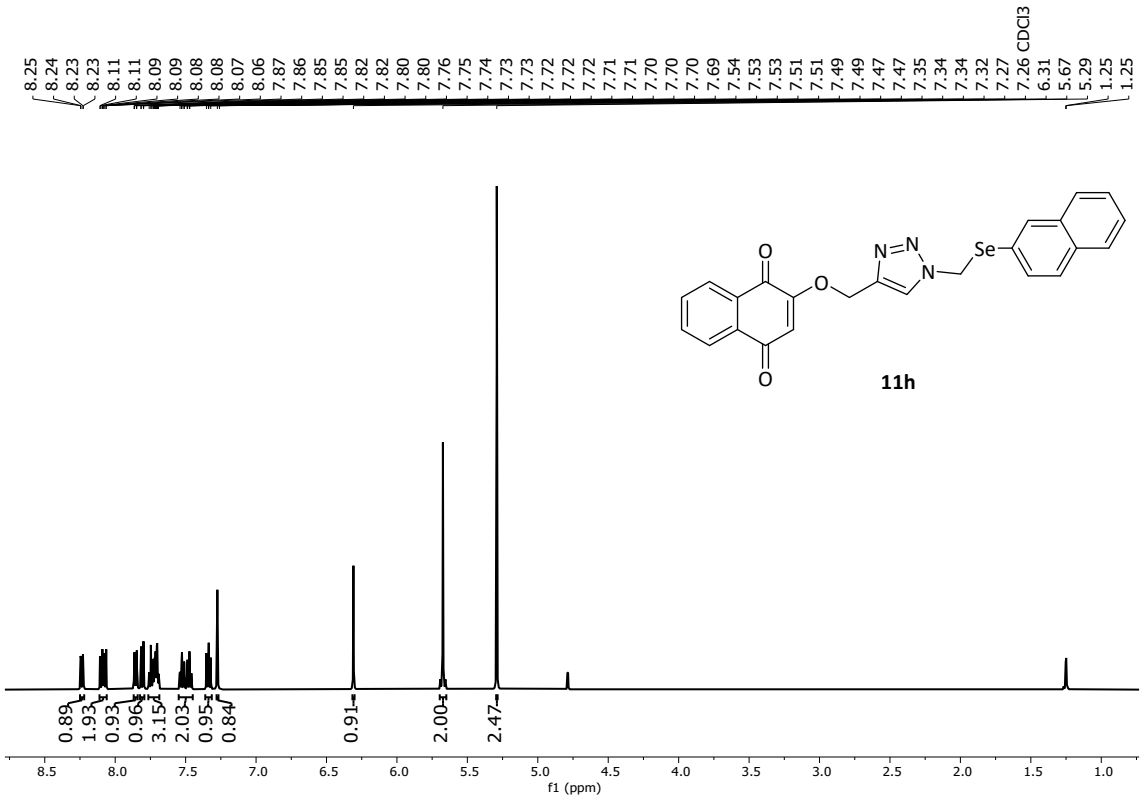

Figure S53. ^{1}H NMR spectrum of compound **11h** in $CDCl_3$ at 500 MHz.

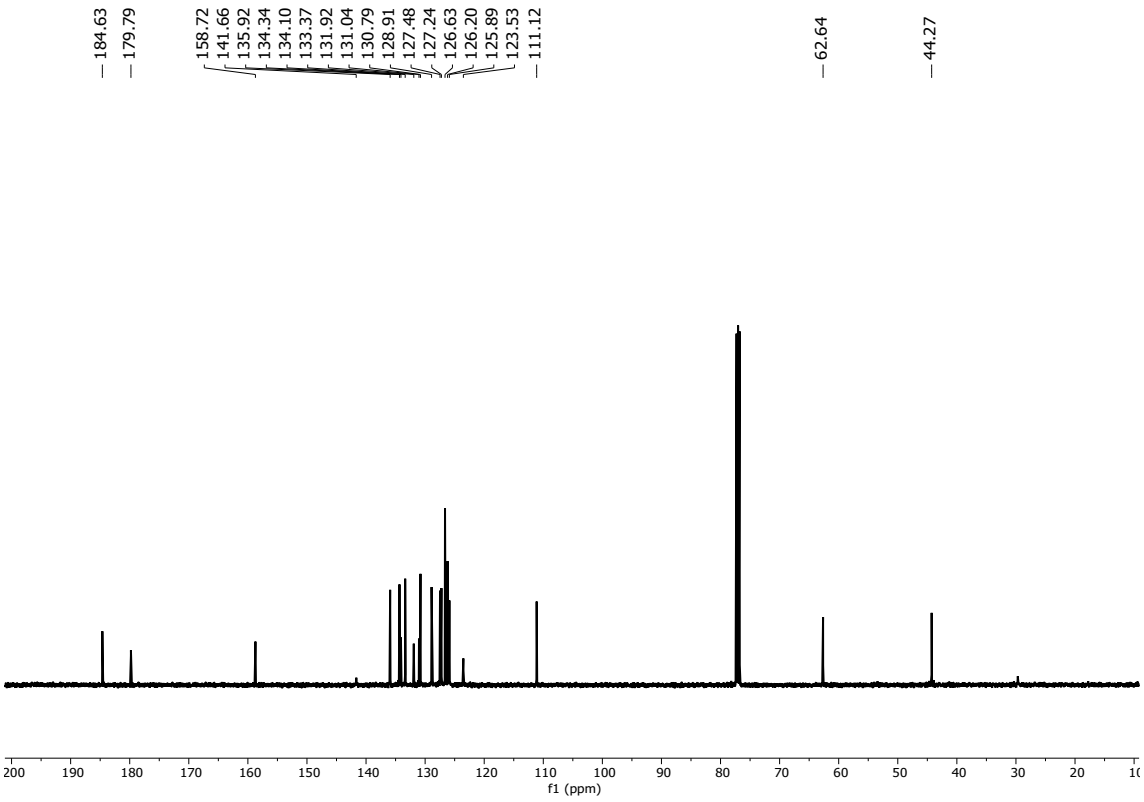

Figure S54. ^{13}C NMR spectrum of compound **11h** in $CDCl_3$ at 125 MHz.

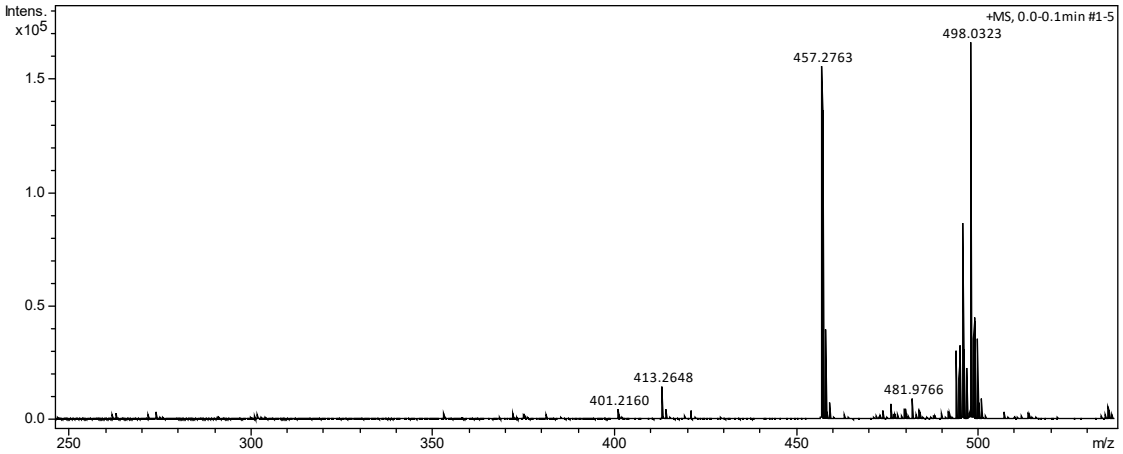

Figure S55. ESI MS spectrum of **11h**.

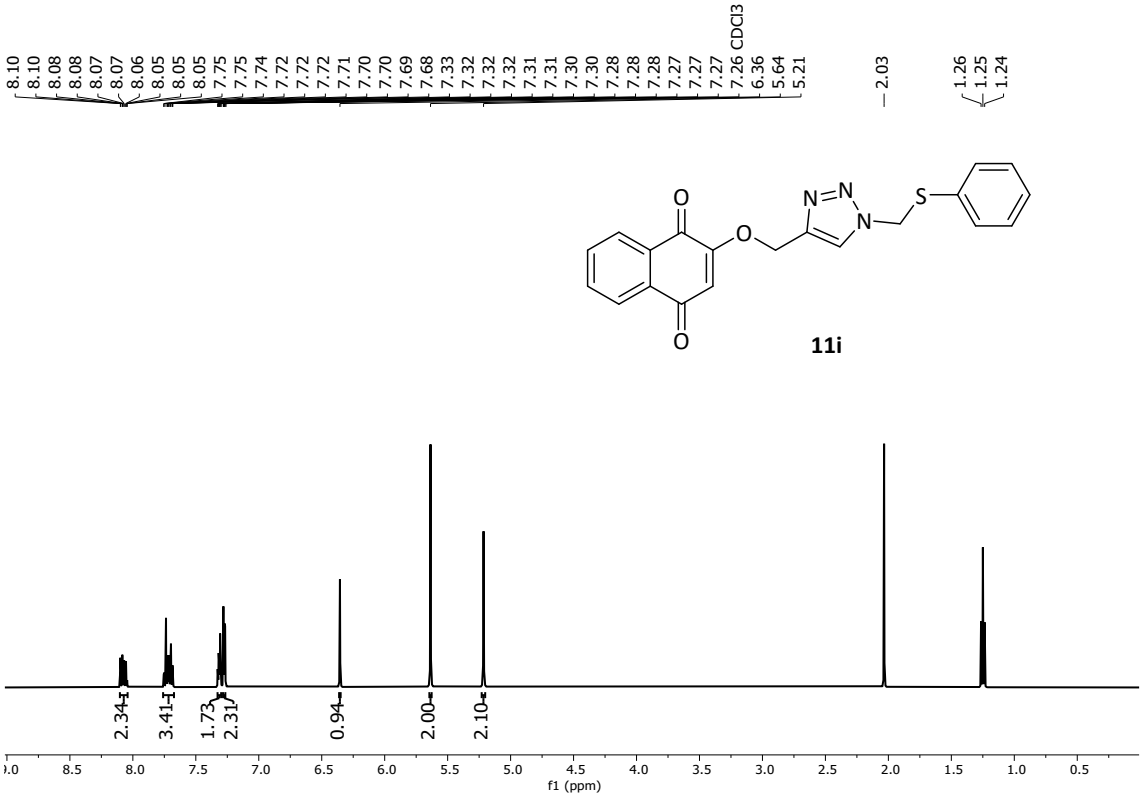

Figure S56. ^{1}H NMR spectrum of compound **11i** in $CDCl_3$ at 500 MHz.

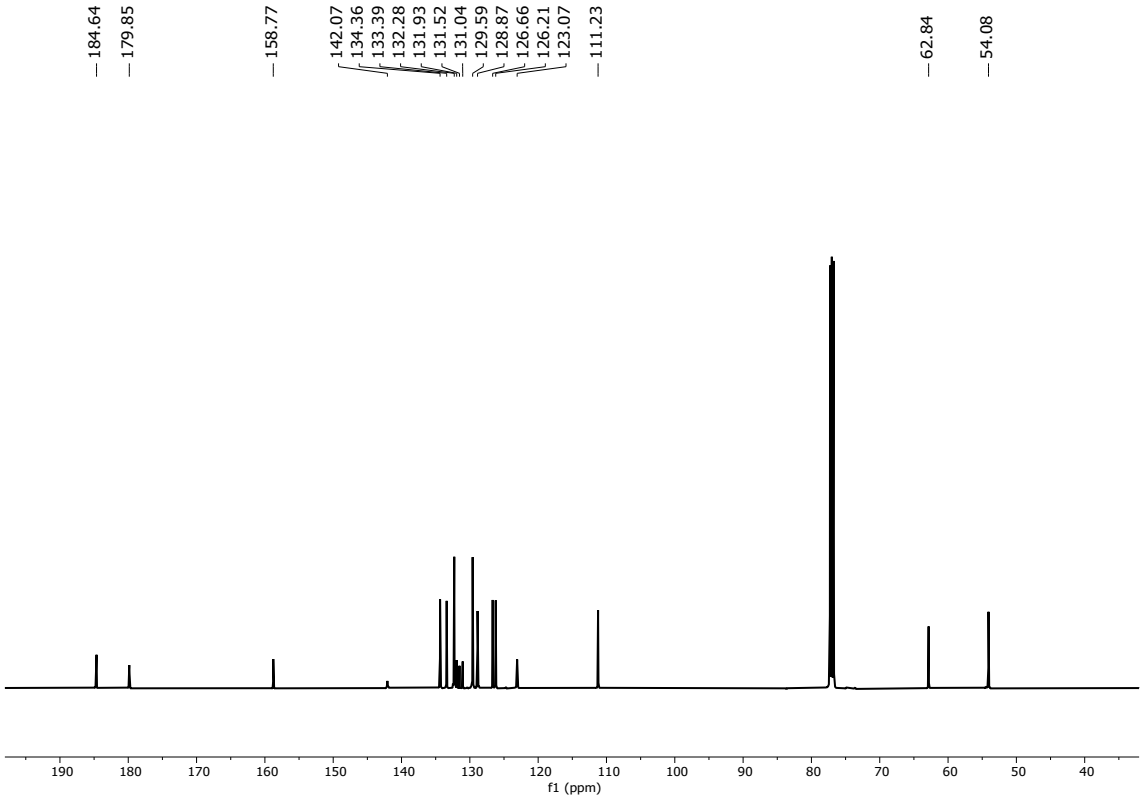

Figure S57. ^{13}C NMR spectrum of compound **11i** in $CDCl_3$ at 125 MHz.

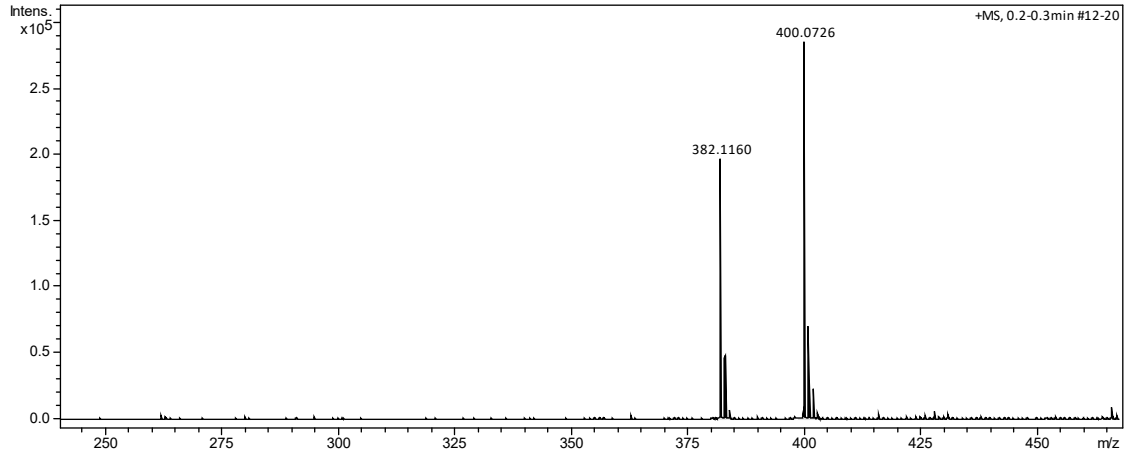

Figure S58. ESI MS spectrum of **11i**.

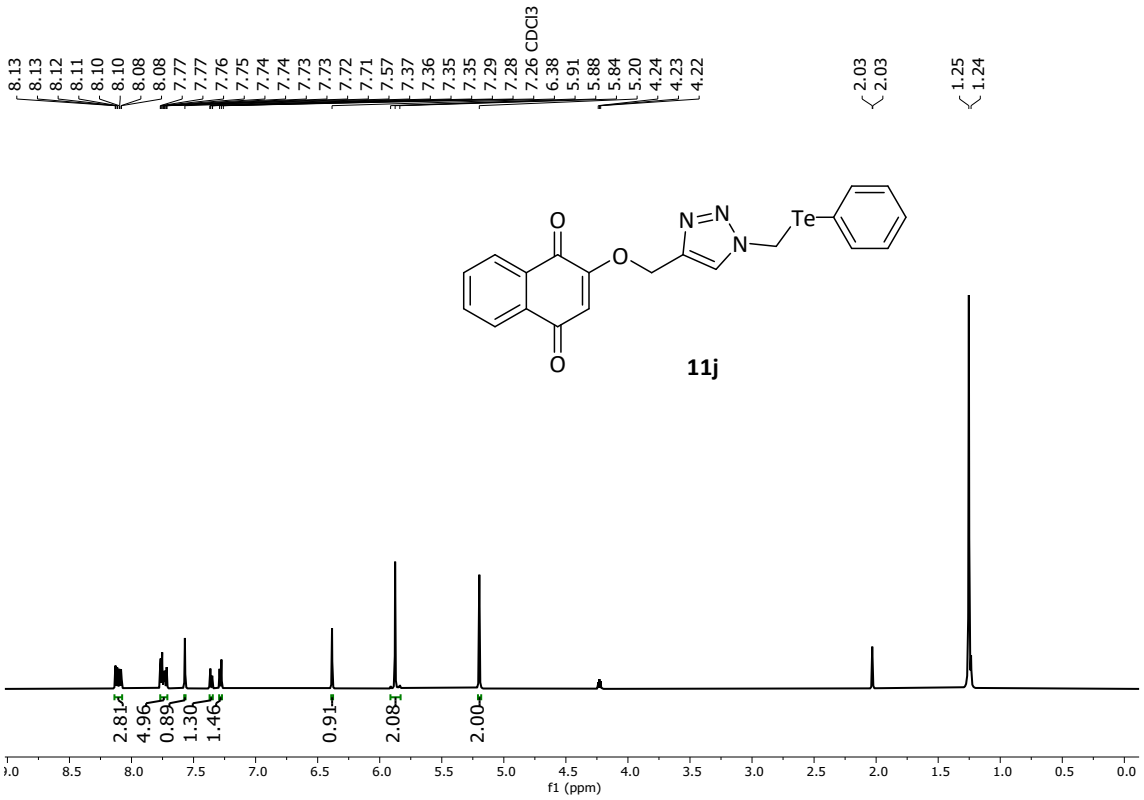

Figure S59. ^{1}H NMR spectrum of compound **11j** in $CDCl_3$ at 500 MHz.

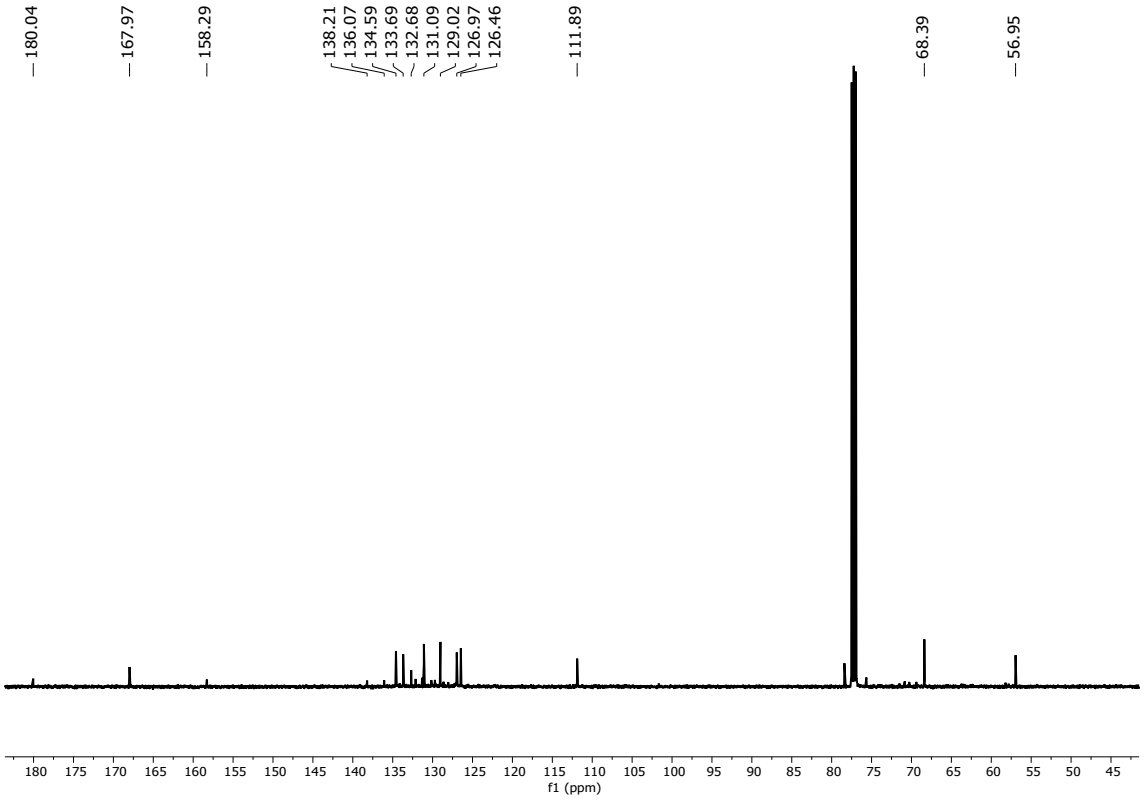

Figure S60. ^{13}C NMR spectrum of compound **11j** in $CDCl_3$ at 125 MHz.

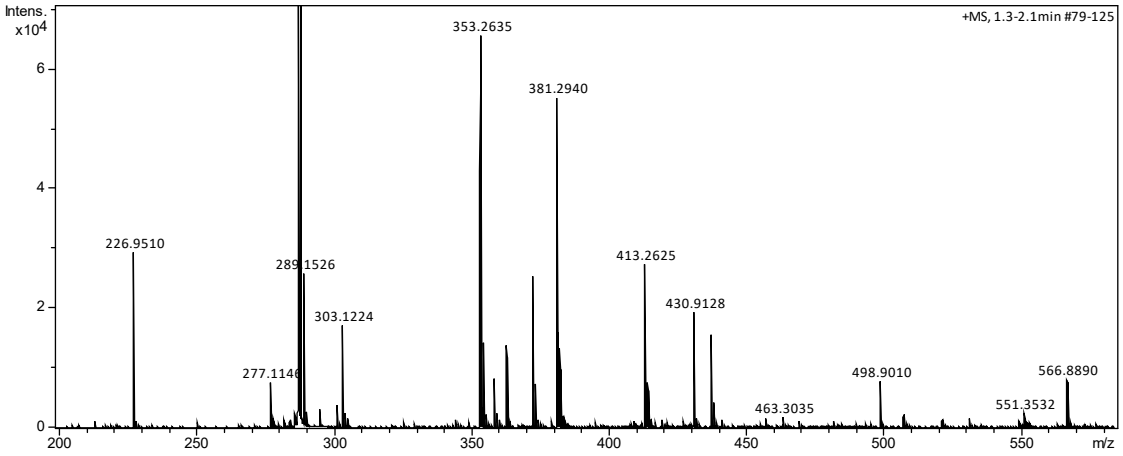

Figure S61. ESI MS spectrum of **11j**.

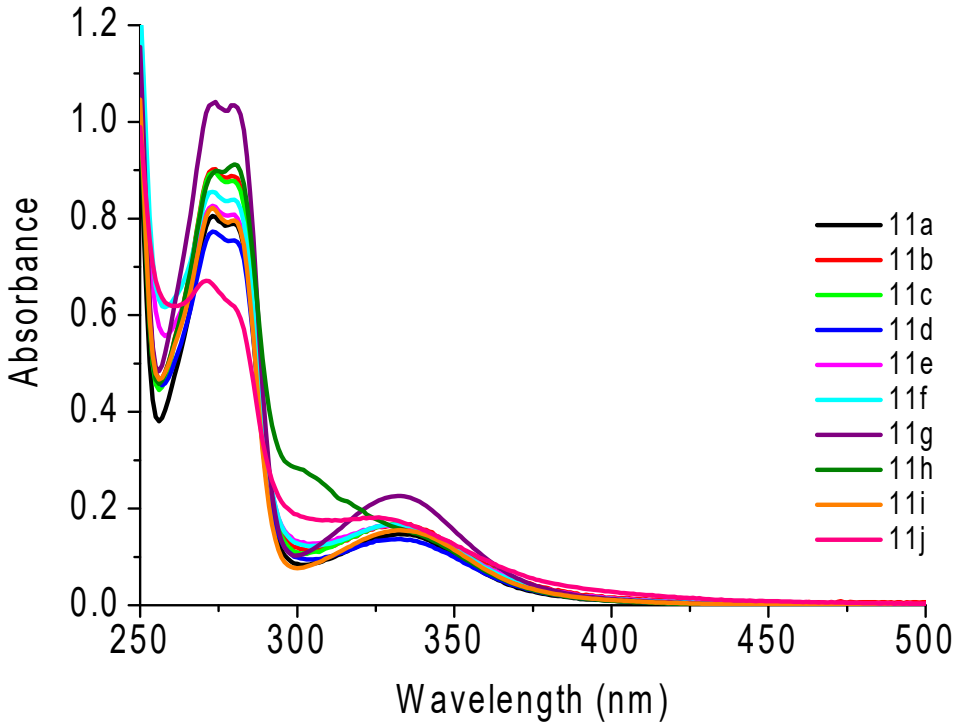

Figure S62. Absorption UV-vis spectra of compounds **11a-j** in DCM solution.

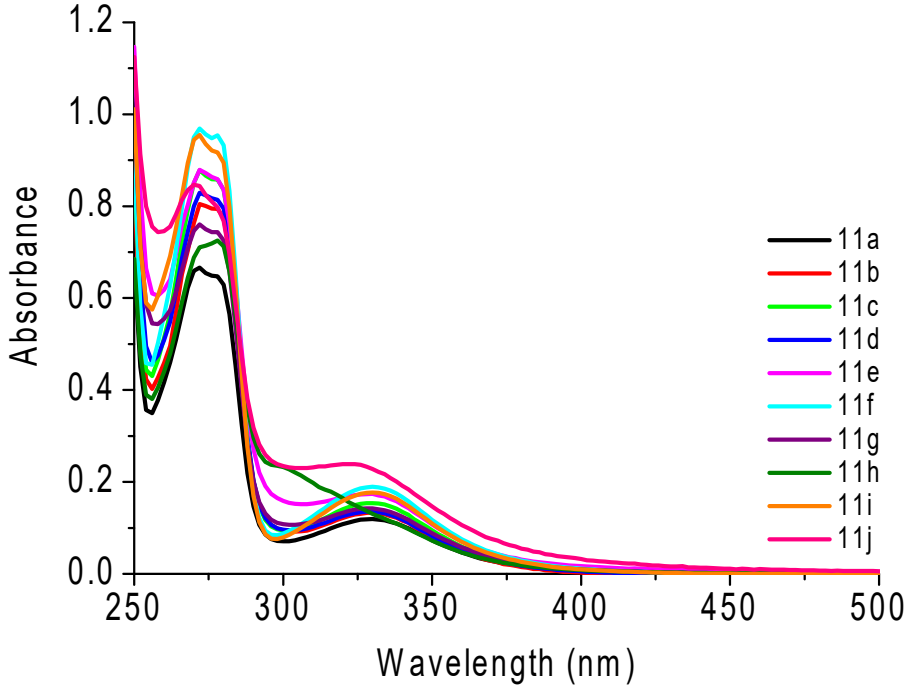

Figure S63. Absorption UV-vis spectra of compounds **11a**-**j** in ACN solution.

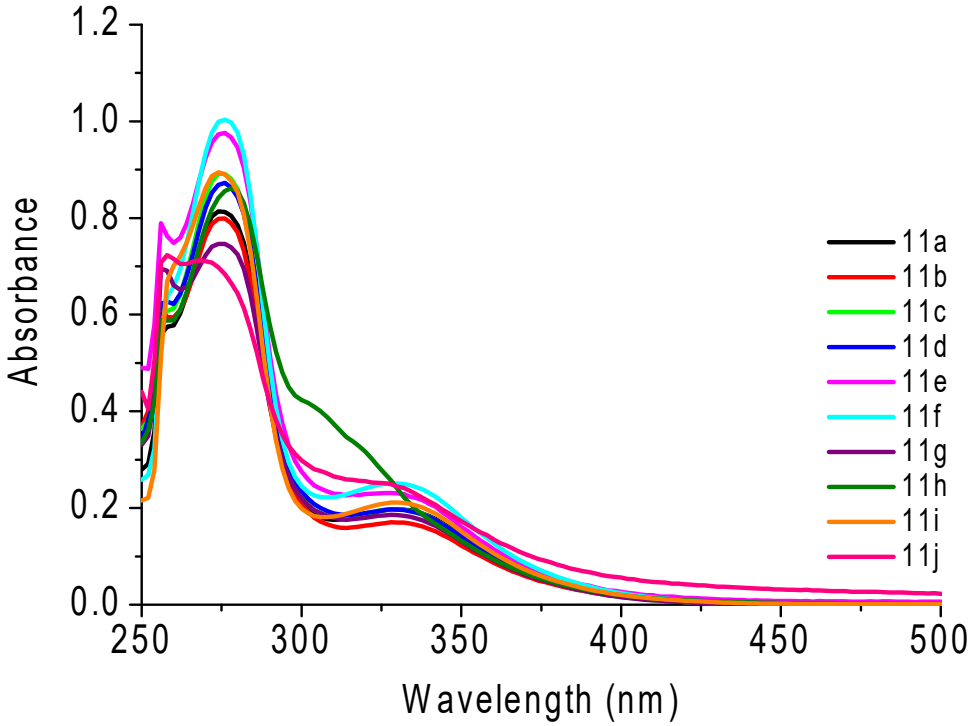

Figure S64. Absorption UV-vis spectra of compounds **11a**-**j** in DMSO solution.

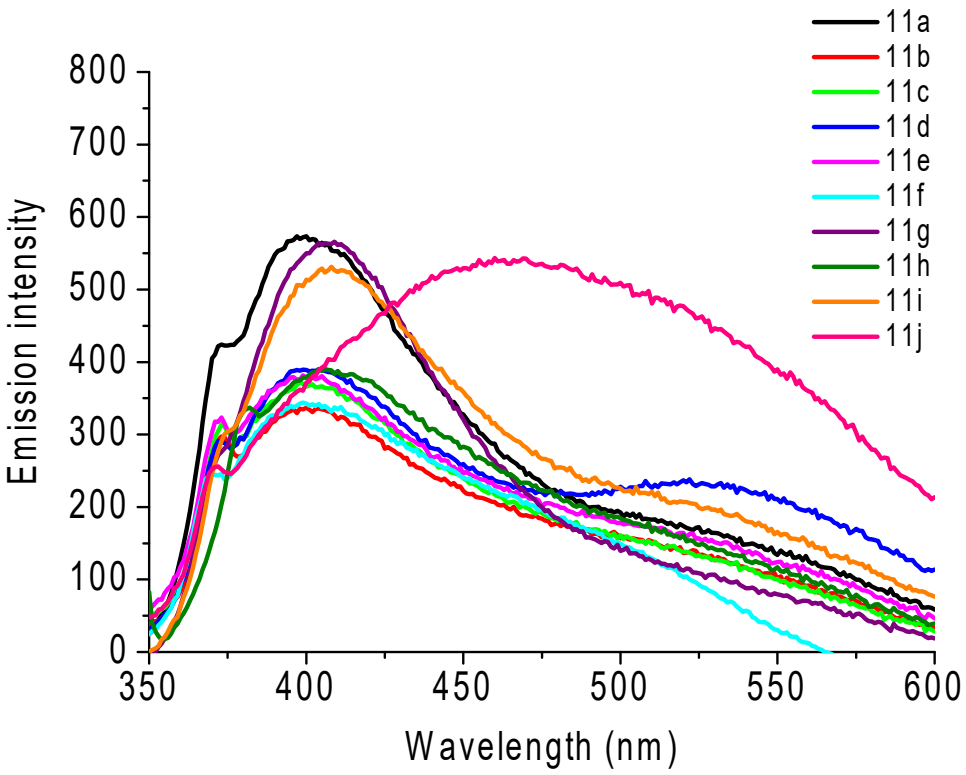

Figure S65. Steady-state fluorescence emission spectra of compounds **11a**-**j** in DCM solution. The compound was excited in the higher energy transition band.

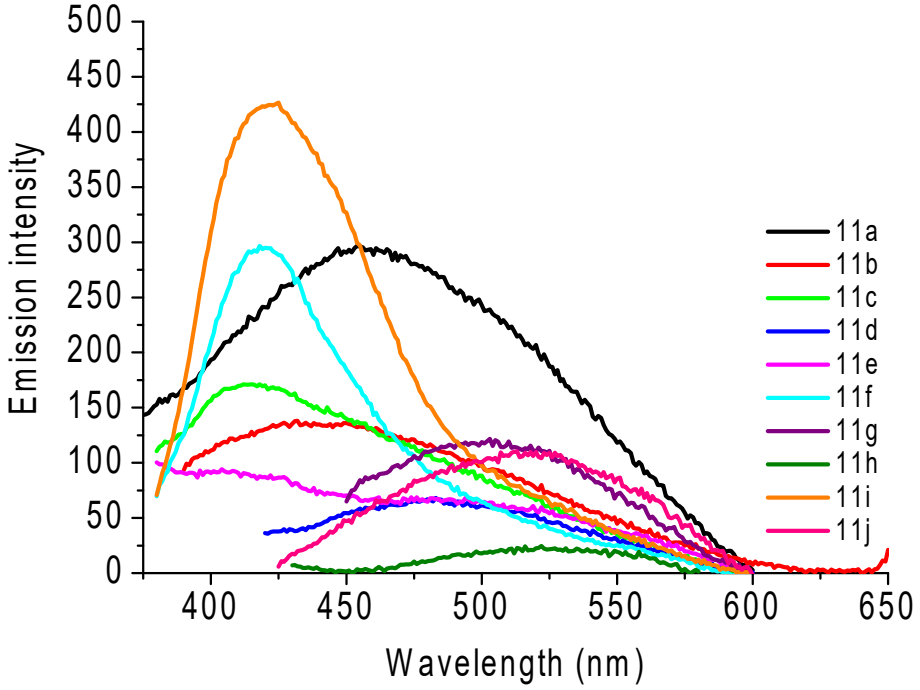

Figure S66. Steady-state fluorescence emission spectra of compounds **11a**-**j** in ACN solution. The compound was excited in the higher energy transition band.

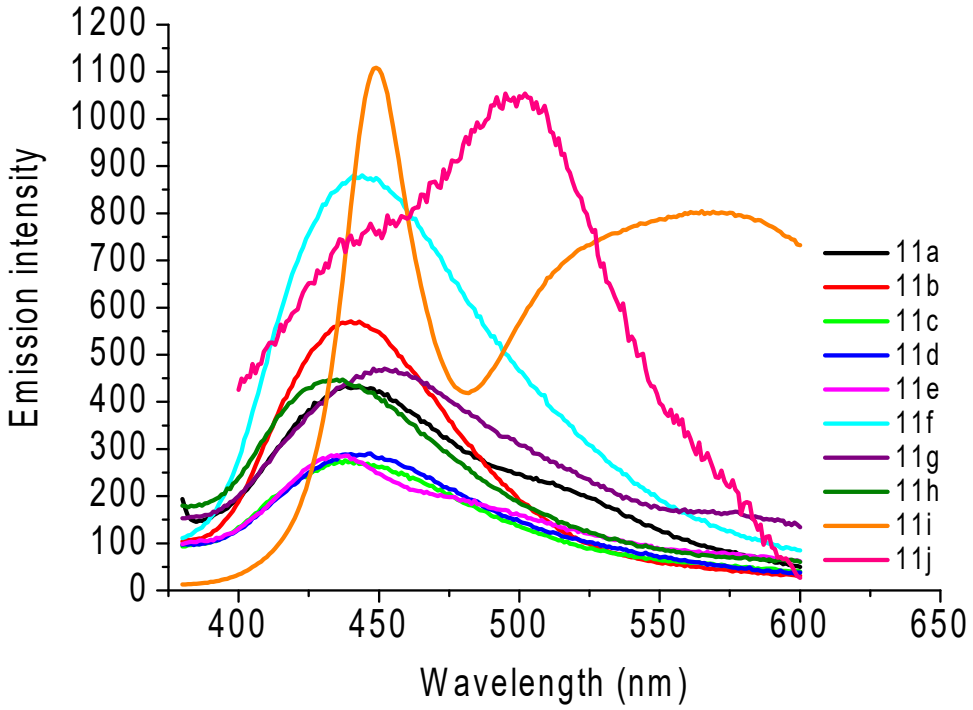

Figure S67. Steady-state fluorescence emission spectra of compounds **11a-j** in DMSO solution. The compound was excited in the higher energy transition band.

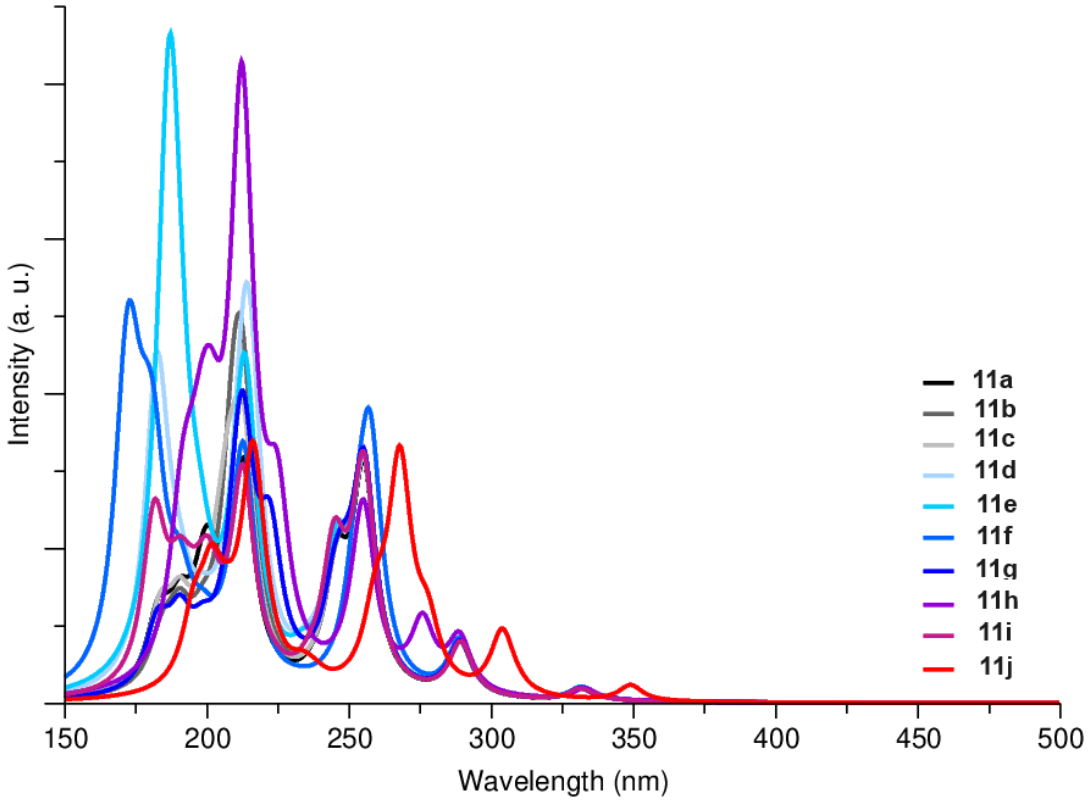

Figure S68. TDDFT optical absorption of compounds **11a-j** in DMSO.

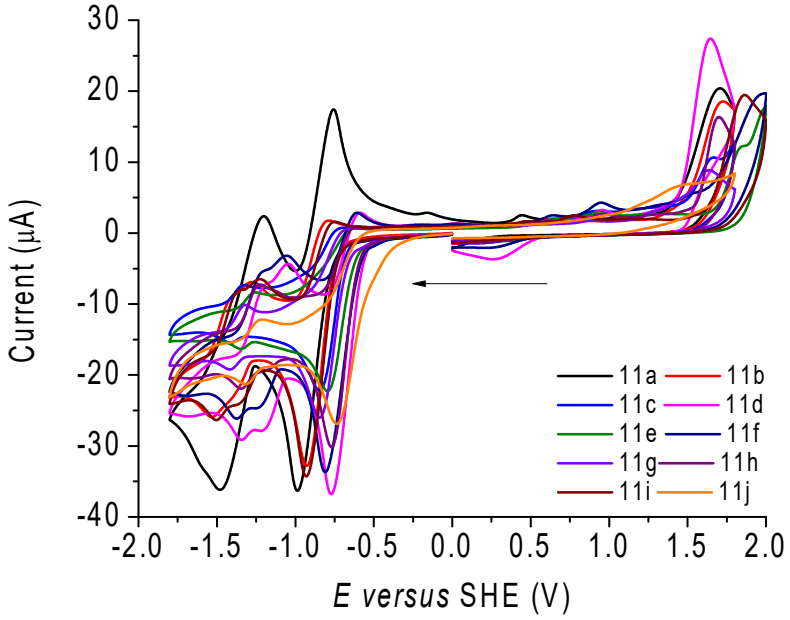

Figure S69. CV analysis of compounds **11a-j** in DCM solution using $TBAPF_6$ as the supporting electrolyte and scan rate at 100 mV/s.

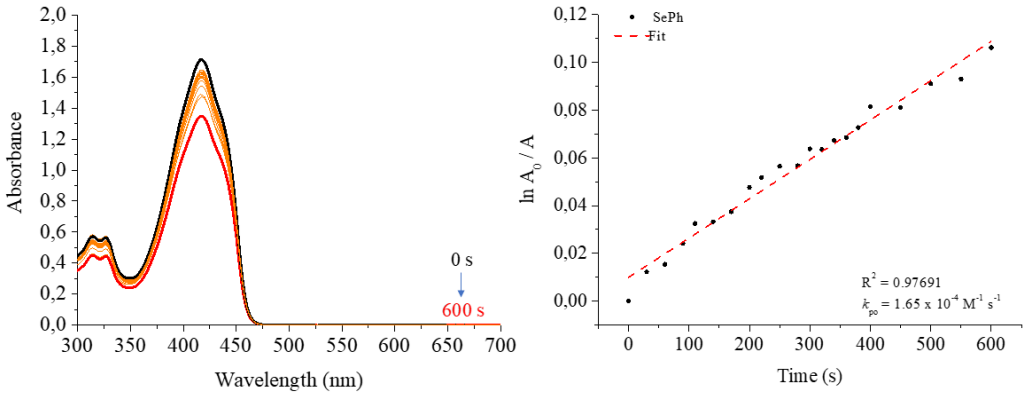

Figure S70. DPBF photo-oxidation assay with compound **11a** in DMSO solution.

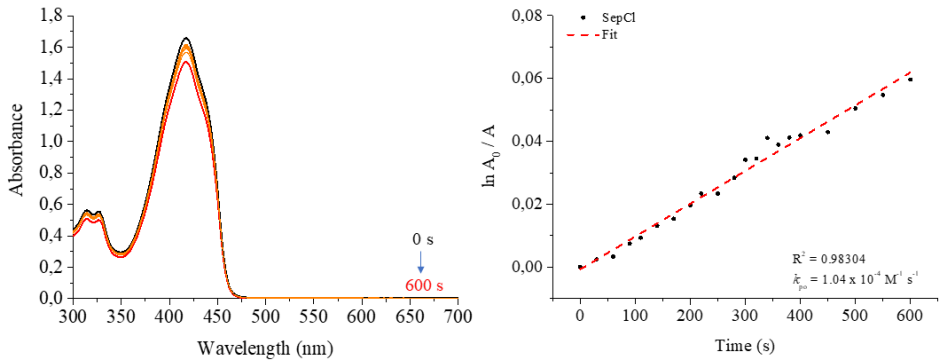

Figure S71. DPBF photo-oxidation assay with compound **11b** in DMSO solution.

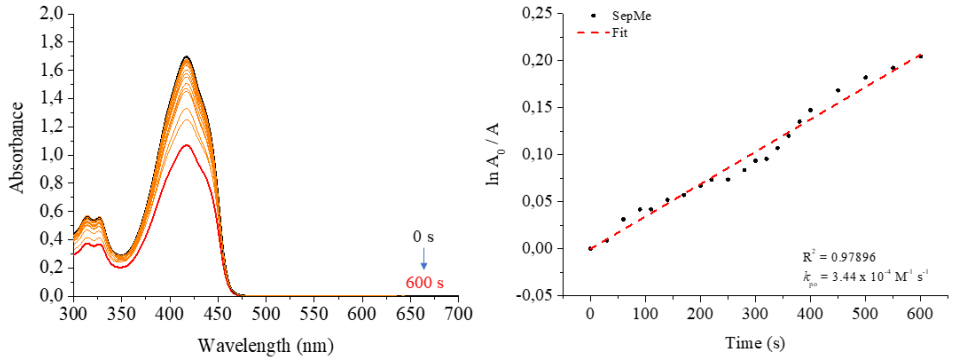

Figure S72. DPBF photo-oxidation assay with compound **11c** in DMSO solution.

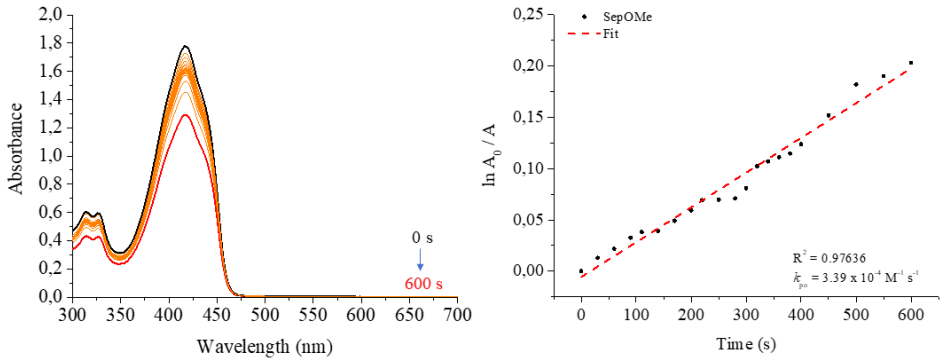

Figure S73. DPBF photo-oxidation assay with compound **11d** in DMSO solution.

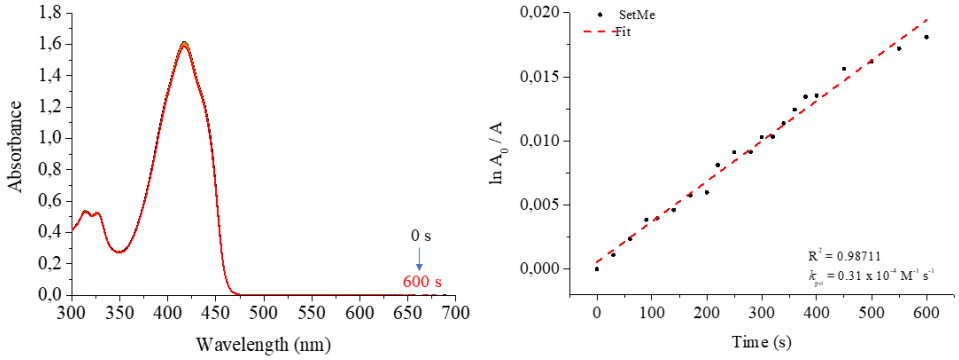

Figure S74. DPBF photo-oxidation assay with compound **11e** in DMSO solution.

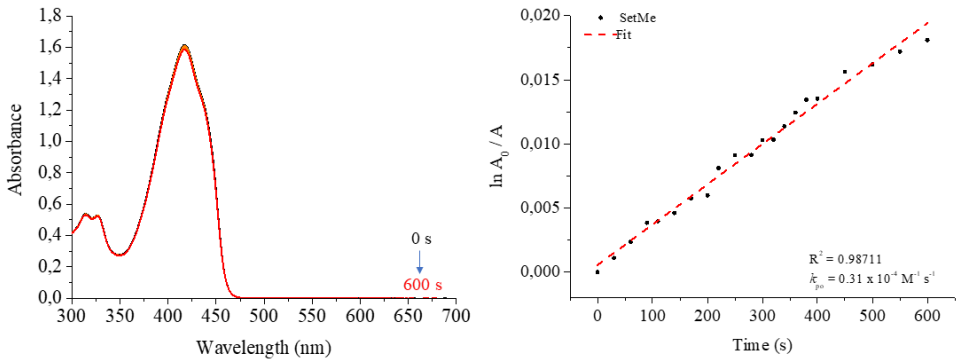

Figure S75. DPBF photo-oxidation assay with compound **11f** in DMSO solution.

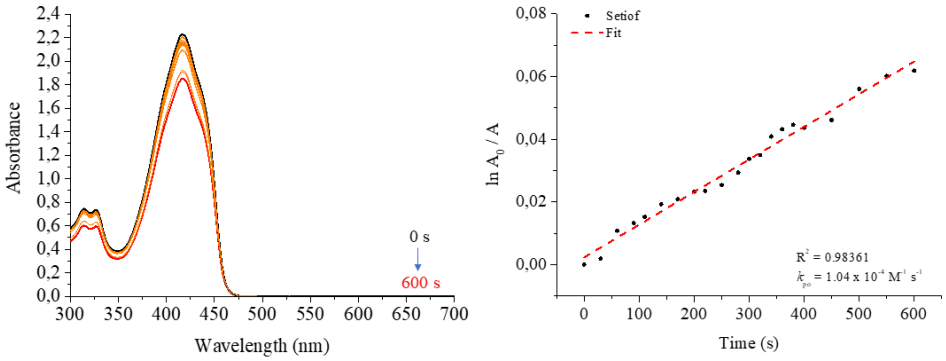

Figure S76. DPBF photo-oxidation assay with compound **11g** in DMSO solution.

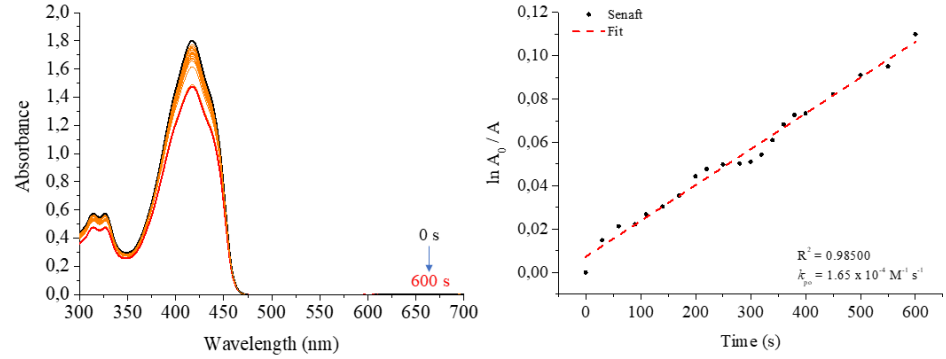

Figure S77. DPBF photo-oxidation assay with compound **11h** in DMSO solution.

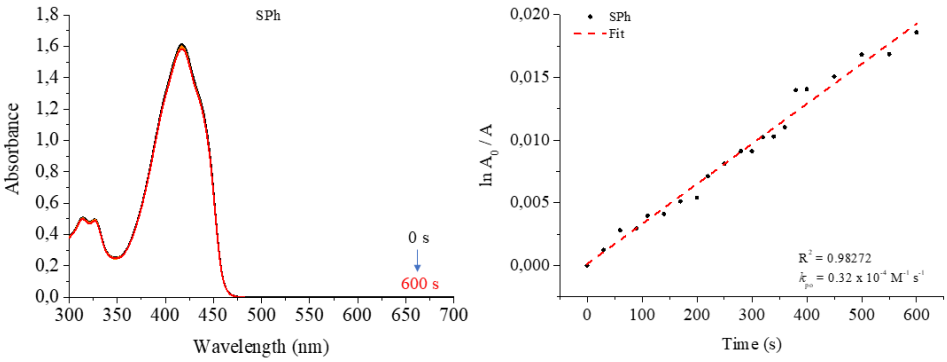

Figure S78. DPBF photo-oxidation assay with compound **11i** in DMSO solution.

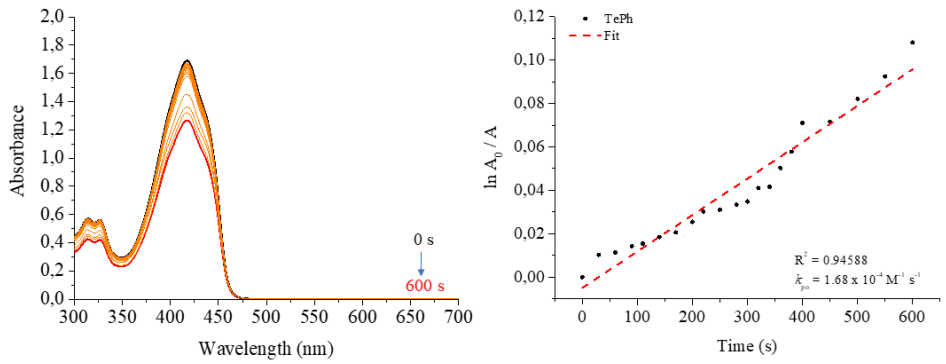

Figure S79. DPBF photo-oxidation assay with compound **11j** in DMSO solution.

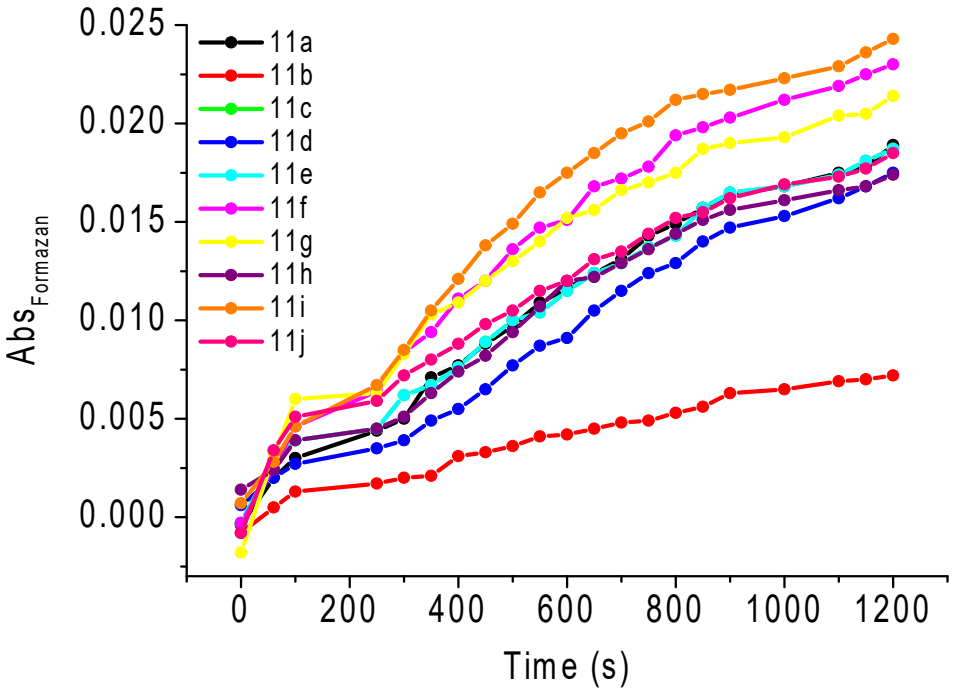

Figure S80. NBT reduction assays of compounds **11a-j** in DMSO solution.

Antioxidant activity evaluation by DPPH analyses

The free radical scavenging ability of derivatives **11a-j** was determined by using the 2,2-diphenyl-1-picrylhydrazyl (DPPH) method. Briefly, a 200 µL solution of 1.0 mM DPPH was mixed with 1.0 mL at different concentrations (50, 100, 150, 200, 250, 300, 350, 400, 450, and 500 µM) of the derivatives **11a-j** in dimethyl sulfoxide (DMSO) solutions. The same concentrations of ascorbic acid (AA) were used as the reference compound. The mixture was mixed thoroughly and kept in the dark at room temperature for 30 min. Then, the absorbance was measured at 517 nm after 30 min of incubation at room temperature to evaluate DPPH reduction. The ability of derivatives **11a-j** to scavenge DPPH radicals was calculated using Equation 1:

$$\%Scavenging\ activity = A_{control} - A_{sample} / A_{control} \times 100\% \quad \textbf{(1)}$$

The radical scavenging potential was expressed as an EC_{50} value and represented the test compound concentration at which 50% of the DPPH radicals are scavenged. All tests were performed in duplicate and the values represented as the mean.